ACS NANO

www.acsnano.org

ARTICLE

Bacterial Growth-Induced Tobramycin Smart Release Self-Healing Hydrogel for *Pseudomonas aeruginosa*-Infected Burn Wound Healing

Ying Huang, Lei Mu, Xin Zhao, Yong Han, and Baolin Guo*

Cite This: *ACS Nano* 2022, 16, 13022−13036

Read Online

ACCESS | Metrics & More | Article Recommendations | Supporting Information

ABSTRACT: **Burns are a common health problem worldwide and are highly susceptible to bacterial infections that are difficult to handle with ordinary wound dressings. Therefore, burn wound repair is extremely challenging in clinical practice. Herein, a series of self-healing hydrogels (QCS/OD/TOB/PPY@PDA) with good electrical conductivity and antioxidant activity were prepared on the basis of quaternized chitosan (QCS), oxidized dextran (OD), tobramycin (TOB), and polydopamine-coated polypyrrole nanowires (PPY@PDA NWs). These Schiff base cross-links between the aminoglycoside antibiotic TOB and OD enable TOB to be slowly released and responsive to pH. Interestingly, the acidic substances during the bacteria growth process can induce the on-demand release of TOB, avoiding the abuse of antibiotics. The antibacterial results showed that the QCS/OD/TOB/PPY@PDA9 hydrogel could kill high concentrations of *Pseudomonas aeruginosa* (PA), *Staphylococcus aureus*, and *Escherichia coli* in a short time and showed a bactericidal effect for up to 11 days in an agar plate diffusion experiment, while showing good *in vivo* antibacterial activity. Excellent and long-lasting antibacterial properties make it suitable for severely infected wounds. Furthermore, the incorporation of PPY@PDA endowed the hydrogel with near-infrared (NIR) irradiation assisted bactericidal activity of drug-resistant bacteria, conductivity, and antioxidant activity. Most importantly, in the PA-infected burn wound model, the QCS/OD/TOB/PPY@PDA9 hydrogel more effectively controlled wound inflammation levels and promoted collagen deposition, vascular generation, and earlier wound closure compared to Tegaderm dressings. Therefore, the TOB smart release hydrogels with on-demand delivery are extremely advantageous for bacterial-infected burn wound healing.**

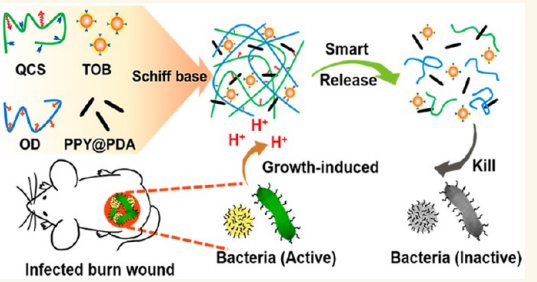

KEYWORDS: *antibiotic smart release hydrogel, burn wound healing, bacterial growth response, on-demand delivery, antibacterial infection*

Burns are the fourth most common destructive trauma worldwide and are prevalent in both military and civilian populations.[1,2] Healing of burn wounds requires the substitution of inactivated tissue, and this is a more delicate and complex process than other wound repair processes.[3,4] Furthermore, burn injuries are highly vulnerable to invasive microbial infections before complete epithelialization, with *Pseudomonas aeruginosa* (PA) and *Staphylococcus aureus* (SA) being the most prevalent microbial infections.[1,2,5] Wound infection will seriously affect the process of wound healing, such as inflammation resolution, epidermal maturation, and neovascularization.[2] Severe infections can even cause complications such as sepsis, which can be life-threatening.[6,7] Therefore, susceptible burn wounds require immediate antimicrobial treatment to prevent complications.[2] The process of healing a burn wound is a lengthy and arduous one. Although many kinds of different wound dressings have been developed for burns in recent years with obvious healing-promoting effects, most of them do not have excellent antibacterial ability to prevent burn wound infection and cannot cope with infected burn wounds.[8−14] Therefore, developing an ideal dressing that can effectively deal with infected burn wounds remains a challenge.

Tobramycin (TOB) can treat various bacterial infections, clinically mainly for serious infections caused by sensitive bacteria, especially those due to Gram-negative bacteria, such

Received: June 7, 2022
Accepted: August 1, 2022
Published: August 3, 2022

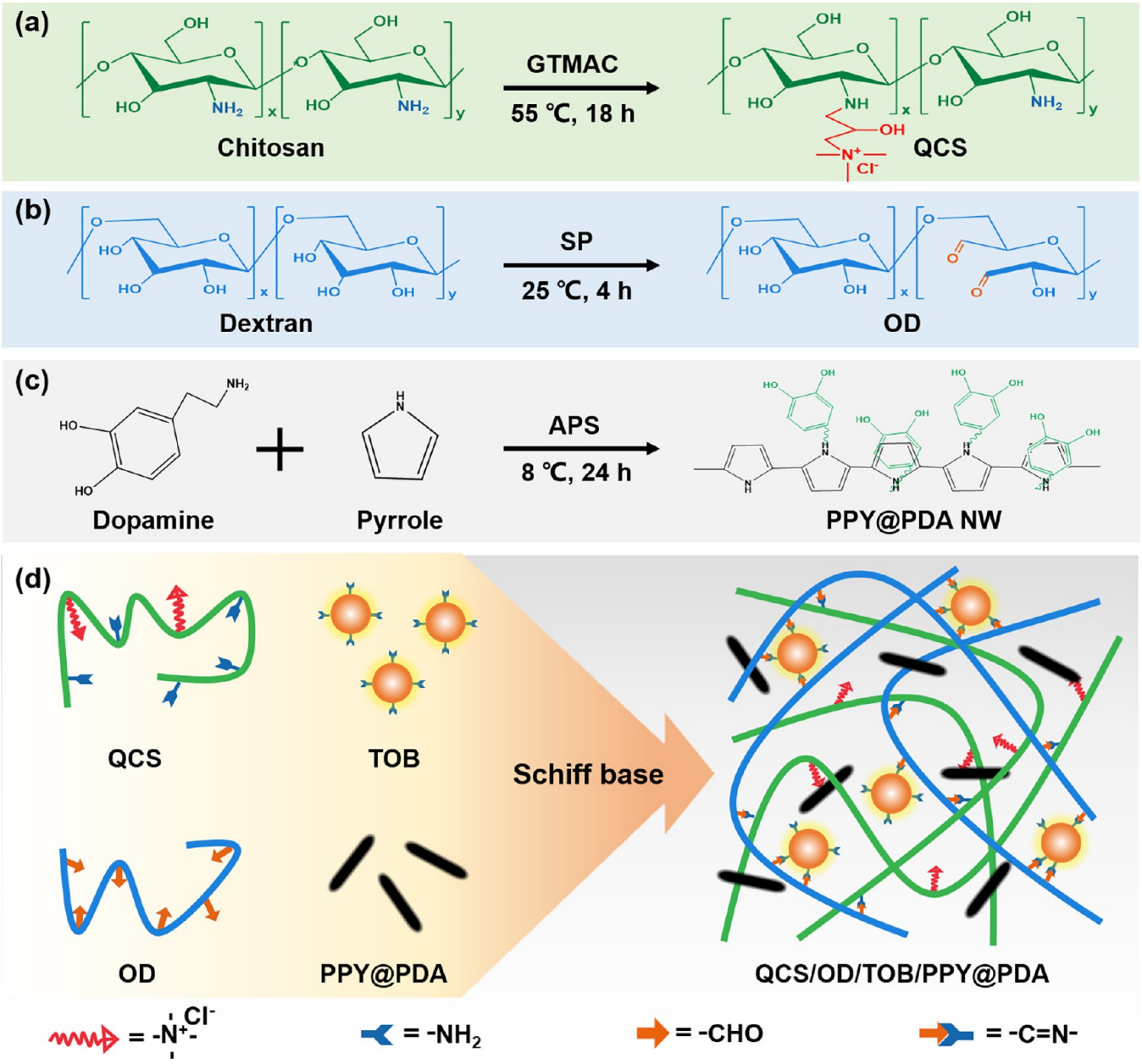

Figure 1. (a) Synthesis of QCS. (b) Synthesis of OD. (c) Synthesis of PPY@PDA NWs. (d) Diagram of QCS/OD/TOB/PPY@PDA hydrogel formation.

as burn infections caused by PA.[15−17] TOB exerts its bactericidal effect by inhibiting bacterial protein synthesis and damaging bacterial cell membranes.[18−20] Although TOB exhibits excellent antibacterial effects, it is a concentration-dependent antibiotic and incorrect or uncontrolled use may cause serious irreversible side effects.[16,18,21] Therefore, the development of a bacterially induced on-demand release TOB hydrogel system is promising for burn wound healing.

On the other hand, chitosan, with good biocompatibility, has abundant medical advantages, such as hemostasis and wound healing ability.[22−24] Quaternized chitosan (QCS) makes up for the poor water solubility of chitosan and provides the ability to resist drug-resistant bacteria.[25−28] In addition, dextran can trigger the body's immune system,[29,30] and it is rich in aldehyde groups after oxidation and can react with QCS to form self-healing hydrogels by Schiff base reaction. TOB belongs to the aminoglycoside antibiotics, and it can be reacted with oxidized dextran (OD) to forming a cross-linked network through Schiff base reaction. Therefore, we hypothesize that loading TOB into the QCS/OD hydrogel system can realize the slow and sustained release of TOB in the physiological environment. Furthermore, the bacteria release acidic substances such as lactic acid and carbonic acid as they grow. Therefore, in the process of bacterial multiplication, the pH-responsive Schiff base hydrogel will rapidly release TOB to eliminate bacteria and protect the wound from infection.[31,32] The bacterial response behavior can precisely control TOB release, which meets the requirement for on-demand drug delivery. Moreover, the incorporation of PPY@PDA nanowires with good electrical conductivity, antioxidant activity, and photothermal behavior further enhanced the wound-healing-promoting ability of the hydrogel.[33−38] Therefore, TOB smart release hydrogels based on QCS and OD and combined with PPY@PDA have significant potential in the repair of PA-

https://doi.org/10.1021/acsnano.2c05557
ACS Nano 2022, 16, 13022−13036

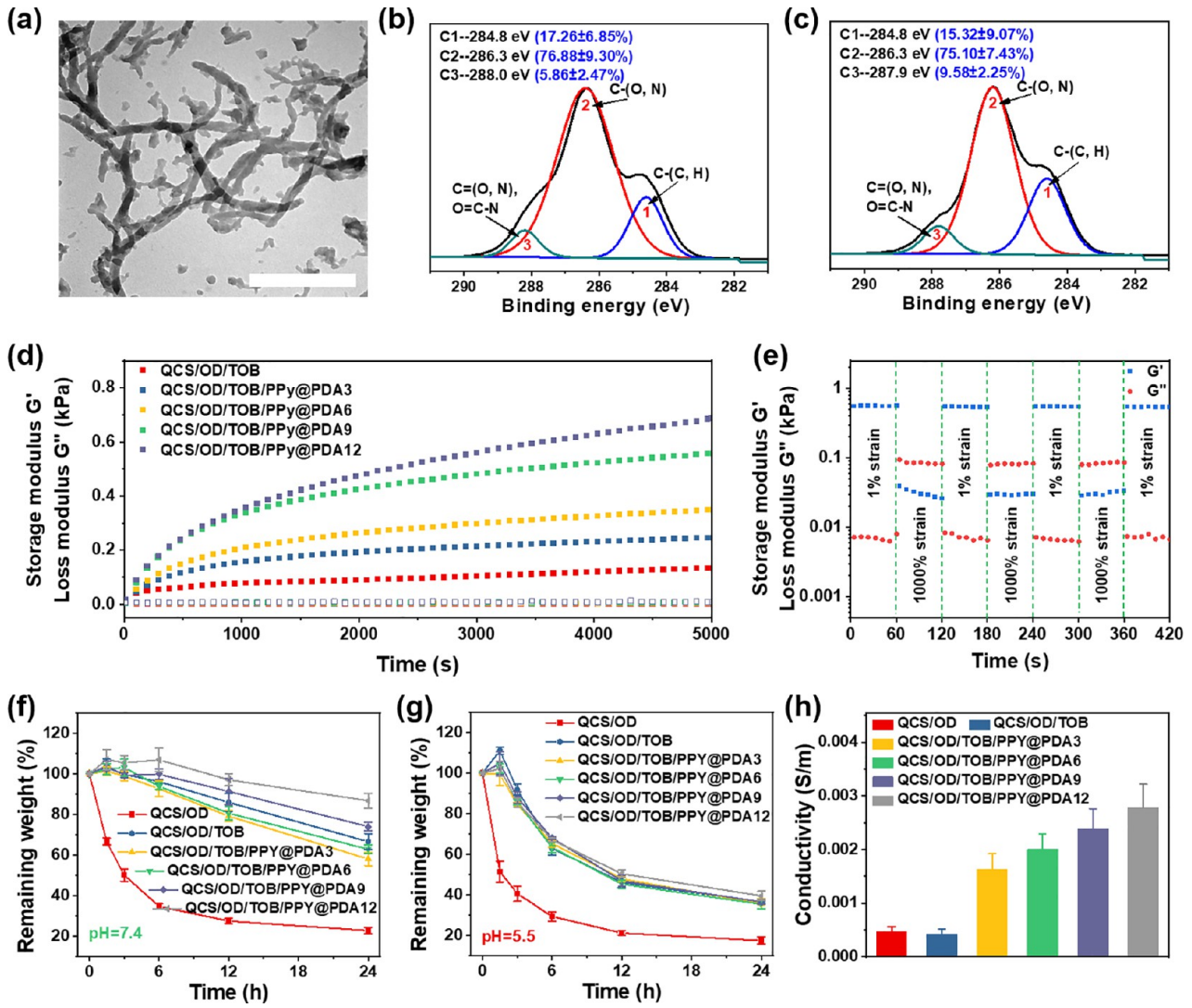

Figure 2. (a) TEM image of PPY@PDA NWs. Scale bar: 500 nm. (b) XPS C 1s spectrum of the QCS/OD hydrogel. (c) XPS C 1s spectrum of the QCS/OD/TOB hydrogel. (d) Rheological behavior of QCS/OD/TOB/PPY@PDA hydrogels. (e) Rheological properties of QCS/OD/TOB/PPY@PDA9 hydrogels. Degradation profiles of QCS/OD/TOB/PPY@PDA hydrogels in PBS with pH = 7.4 (f) and pH = 5.5 (g) at 37 °C. (h) Conductivity of QCS/OD/TOB/PPY@PDA hydrogels.

infected burn wounds, but such dressings have not been reported.

The objective of this study is to develop a self-healing hydrogel with outstanding antibacterial ability through bacterially regulated TOB smart release based on QCS for treating burn wounds. The biocompatibility on this hydrogel was assessed by blood compatibility, cytocompatibility, and *in vivo* host response. The TOB-releasing antibacterial ability of the hydrogel in liquid and solid environments was tested, and its ability to deal with drug-resistant bacteria was evaluated. Finally, the ability of QCS/OD/TOB/PPY@PDA hydrogels to deal with severe wound infection and to promote healing was evaluated by a PA-infected burn wound model. This study will provide a strategy for treating infected burn wounds.

RESULTS AND DISCUSSION

Preparation of the TOB Smart Release Hydrogel. We aimed to develop an antibiotic smart release hydrogel to treat burn wounds susceptible to bacterial infection. First, we selected TOB, which has an excellent bactericidal effect on PA, as the releasing antibiotic.[39] Then, we modified chitosan with abundant biomedical advantages using glycidyltrimethylammonium chloride (GTMAC) to synthesize QCS with better water solubility than chitosan, which could effectively deal with drug-resistant bacteria (Figure 1a).[40] Natural polysaccharide dextran was oxidized through sodium periodate (SP) to obtain multiple aldehyde groups (Figure 1b).[41] QCS with amino groups and OD with multiple aldehyde groups serve as the basic skeleton structure of the hydrogels through Schiff base reaction (QCS/OD hydrogel). TOB with multiple amino groups can also undergo Schiff base reactions with OD as a small-molecule cross-linker (QCS/OD/TOB hydrogel), and this enables TOB to be slowly released and responsive to pH. Meanwhile, the incorporation of TOB improves the toughness and self-healing properties of the hydrogel. In the QCS/OD/TOB hydrogel, the sum of the amino groups of QCS and TOB approximately equals the number of aldehyde groups of OD. Table S1 shows the number of free amino or aldehyde groups of each component per mL of hydrogel. Furthermore, in order to impart photothermal activity, antioxidant activity, and electrical conductivity to the hydrogels, we prepared PPY@PDA nanowires (NWs) by ammonium

https://doi.org/10.1021/acsnano.2c05557
ACS Nano 2022, 16, 13022−13036

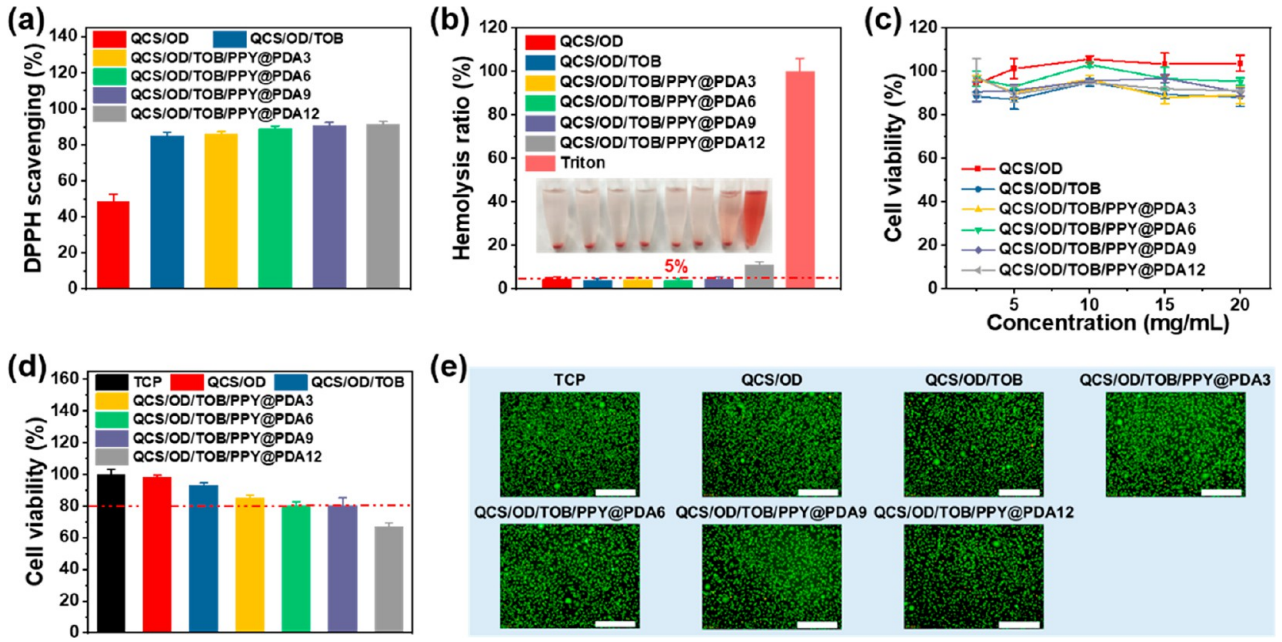

Figure 3. (a) Antioxidant activity of QCS/OD/TOB/PPY@PDA hydrogels. (b) Hemolysis ratio of QCS/OD/TOB/PPY@PDA hydrogels. The cell viability of L929 cells with QCS/OD/TOB/PPY@PDA hydrogel extract culturing (c) and when L929 cells are in contact with the hydrogels for 24 h (d). (e) Live/dead staining of L929 cells after contacting with QCS/OD/TOB/PPY@PDA hydrogels for 24 h. Scale bar: 400 μm.

persulfate (APS)-initiated oxidative polymerization of dopamine and pyrrole (Figure 1c) and prepared hydrogels with different PPY@PDA contents.[42] The PPY@PDA NWs were uniformly dispersed in the hydrogel through hydrogen bonding with QCS and OD. These hydrogels were named QCS/OD/TOB/PPY@PDA*n*, where *n* indicates the concentration of PPY@PDA in the hydrogel as mg/mL. The preparation of the hydrogel is shown in Figure 1.

Characterizations of the Hydrogels. The transmission electron microscope (TEM) image shown in Figure 2a confirms the successful preparation of PPY@PDA NWs. The results showed that the diameter of PPY@PDA NWs is between 40 and 70 nm and the length is about 1 μm, which is consistent with the reported literature.[42] Fourier transform infrared spectroscopy (FT-IR) spectra and X-ray photoelectron spectroscopy (XPS) test results also confirmed the successful preparation of PPY@PDA (Figure S1). In addition, in order to prove that TOB successfully undergoes Schiff base reaction with OD, the chemical structures of the QCS/OD hydrogel and QCS/OD/TOB hydrogel were analyzed by XPS. Figure 2b,c show that the polysaccharide-based hydrogels contain a large number of C2 (C−O). Furthermore, the C 1s spectra of QCS/OD/TOB hydrogels showed an increase in C3 (C═N) content and a decrease in C2 (C−N) content compared to QCS/OD hydrogels because Schiff base bonds increase in the hydrogel system after the introduction of TOB.[43] The N 1s spectra of hydrogels (Figure S2) showed that the peak around 398.6 eV in the QCS/OD hydrogel is pyridine nitrogen (C═N), corresponding to the Schiff base bond in the hydrogel, while the peak around 401.8 eV is quaternary ammonium nitrogen (protonated nitrogen), corresponding to the quaternary ammonium group in the QCS.[44−47] In addition, with the addition of TOB to the hydrogel system, the Schiff base bonds increase and the proportion of quaternary ammonium decreases relatively, so the content of N1 in the QCS/OD/TOB hydrogels increases while the content of N3 decreases. The above results showed that TOB was successfully encapsulated in the hydrogel by Schiff base reaction, and the TOB smart release hydrogel was successfully prepared.

Medical hydrogels should have suitable mechanical strength, and the storage modulus (G') and self-healing properties of hydrogels were tested by rotational rheometer. Figure 2d,e and Figure S3 show that although the QCS/OD hydrogel has the highest storage modulus up to 10 kPa, the QCS/OD hydrogel is fragile, showing poor self-healing performance. After adding TOB, the self-healing property of the hydrogel is greatly improved. In addition, the storage modulus of the hydrogels was enhanced after the incorporation of PPY@PDA and increased with the increase of PPY@PDA content. Except for the QCS/OD/TOB/PPY@PDA12 hydrogel, the QCS/OD/TOB/PPY@PDA hydrogels still have excellent self-healing properties. The above results indicate that TOB improves the flexibility of the hydrogel, and PPY@PDA enhances the mechanical strength of the hydrogel.

Hydrogels based on Schiff base bonds exhibit pH-dependent degradation behavior.[48] Physiological microenvironments (phosphate-buffered saline [PBS], pH = 7.4) and slightly acidic microenvironments (PBS, pH = 5.5) were used to evaluate the degradability of the hydrogels. The results in Figure 2f,g show that the mass loss of the QCS/OD/TOB/PPY@PDA9 hydrogel is about 26% after 24 h of incubation in the physiological microenvironment. However, the mass loss of QCS/OD/TOB/PPY@PDA9 hydrogels was as high as 63% after 24 h of incubation in a slightly acidic microenvironment. Clearly, the hydrogel degrades faster in the slightly acidic microenvironment than in the physiological microenvironment. The above results indicate that the degradation rate of Schiff base hydrogels can be regulated by adjusting the environmental acidity.

Electroactive polymers, such as polypyrrole, can modulate the activity of electrically excited cells, and conductive

https://doi.org/10.1021/acsnano.2c05557
ACS Nano 2022, 16, 13022−13036

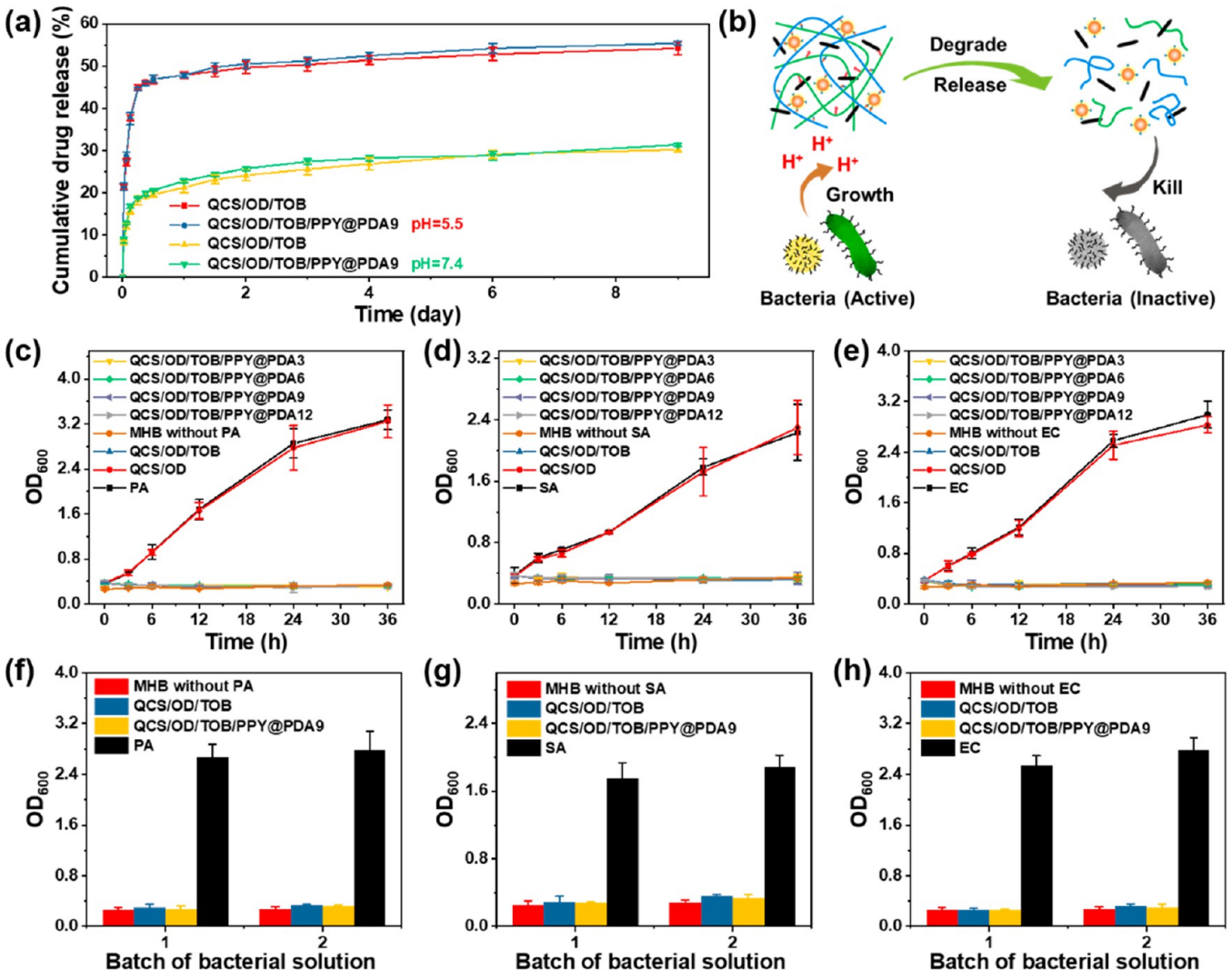

Figure 4. (a) Controlled release profiles of the QCS/OD/TOB hydrogel and QCS/OD/TOB/PPY@PDA9 hydrogel for TOB at pH = 7.4 and pH = 5.5. (b) Mechanism of bacterial growth promoting a TOB bactericidal activity. Growth curves of 10^7 CFU/mL PA (c), SA (d), and EC (e) after different hydrogel treatments. Batches of QCS/OD/TOB hydrogel and QCS/OD/TOB/PPY@PDA9 hydrogel killed 10^7 CFU/mL PA (f), SA (g), and EC (h).

materials were proved to enhance wound healing.[49,50] Therefore, the conductivity of the QCS/OD/TOB/PPY@PDA hydrogel was tested by a digital multimeter. The results in Figure 2h showed that the QCS/OD hydrogel and the QCS/OD/TOB hydrogel possess lower electrical conductivity, about 0.0004 S/m. However, the conductivity of the hydrogel increased significantly after incorporating PPY@PDA NWs. The conductivity of the QCS/OD/TOB/PPY@PDA3 hydrogel reaches 0.0016 S/m, which is 4 times that of the hydrogel without PPY@PDA. With the increase of PPY@PDA content, the electrical conductivity of the hydrogel keeps increasing, and QCS/OD/TOB/PPY@PDA12 has the highest electrical conductivity, which is 0.0028 S/m, while the conductivity of QCS/OD/TOB/PPY@PDA9 is 0.0024 S/m. The above results showed that the incorporation of PPY@PDA can effectively improve the electrical conductivity of the hydrogel.

Antioxidant Activity of the Hydrogel. Dressings with antioxidant activity can regulate the content of reactive oxygen species around the wound to promote wound healing.[51,52] Its antioxidant activity was evaluated by testing the scavenging efficiency of the QCS/OD/TOB/PPY@PDA hydrogel for 1, 1-diphenyl-2-picrylhydrazyl (DPPH). The results in Figure 3a showed that the QCS/OD hydrogel has a scavenging ratio of 48% for DPPH, which is because of the combined action of the free aldehyde groups and QCS of the QCS/OD hydrogel.[40,53,54] After the incorporation of TOB into the hydrogel, the scavenging ratio of the QCS/OD/TOB hydrogel for DPPH increased to 85%. In addition, the antioxidant efficiency of the hydrogels was further enhanced after incorporating PPY@PDA and increased with the increase of PPY@PDA content, among which the DPPH scavenging ratio of the QCS/OD/TOB/PPY@PDA9 hydrogel and QCS/OD/TOB/PPY@PDA12 hydrogel is over 90%. Therefore, CS/OD/TOB/PPY@PDA hydrogels exhibit good antioxidant activity, which is beneficial for wound healing.

Biocompatibility of the Hydrogel. Good biocompatibility is the basic requirement of medical dressings.[55,56] Hemocompatibility testing and cytocompatibility testing are the most common methods for evaluating the biocompatibility of hydrogel materials.[57] Figure 3b shows the results of hemocompatibility. Except that the hemolysis ratio of CS/OD/TOB/PPY@PDA12 hydrogel is 11%, the hemolysis ratios

https://doi.org/10.1021/acsnano.2c05557
ACS Nano 2022, 16, 13022−13036

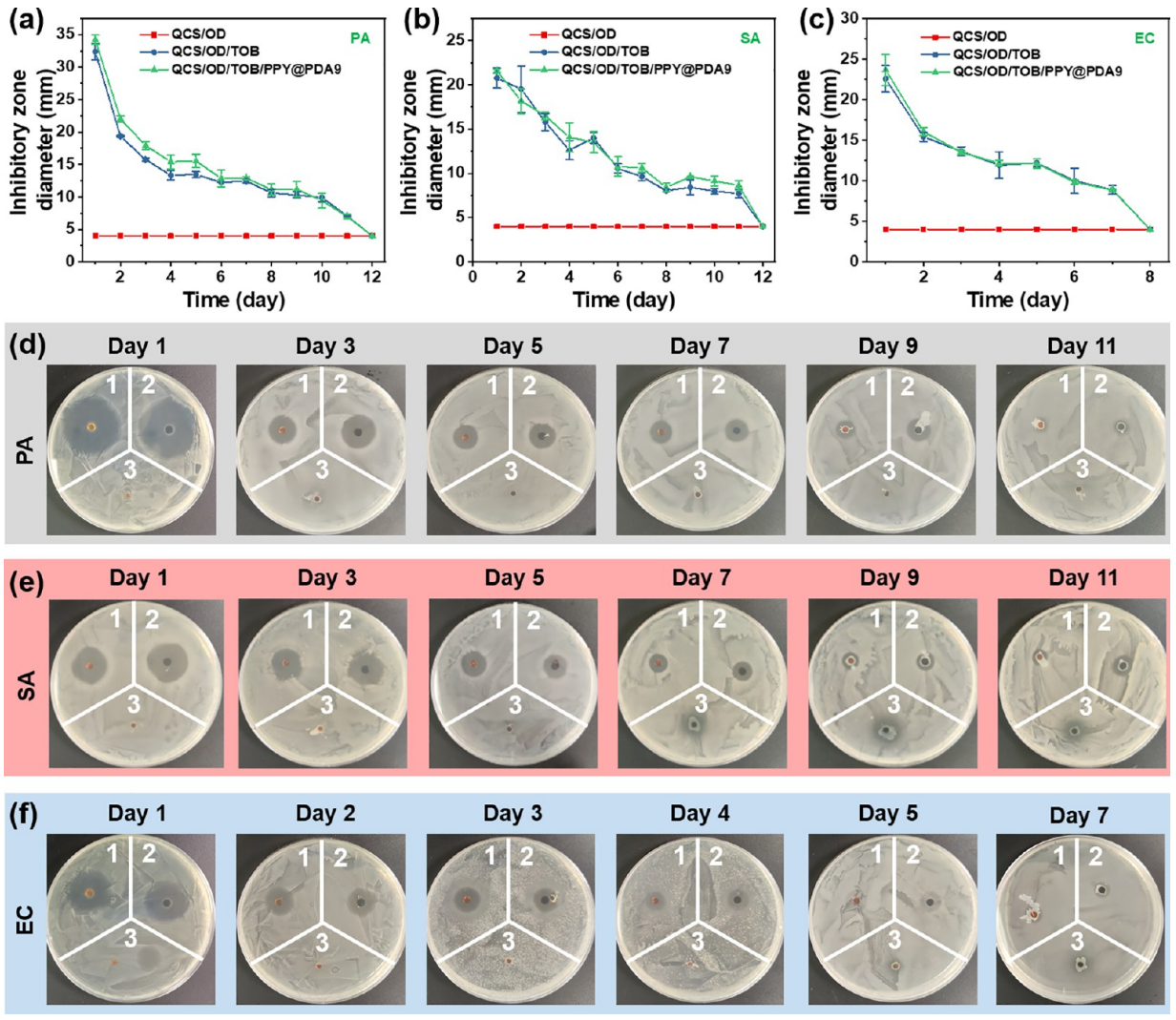

Figure 5. Inhibition zone diameters of (a) PA, (b) SA, and (c) EC. Pictures of inhibition zones of (d) PA, (e) SA, and (f) EC (1 for QCS/OD/TOB, 2 for QCS/OD/TOB/PPY@PDA9, and 3 for QCS/OD).

of other CS/OD/TOB/PPY@PDA hydrogels are all within 5%. Similarly, the macroscopic photos of the hemolysis experiment showed that the positive control Triton was bright red, while the CS/OD/TOB/PPY@PDA12 hydrogel was slightly reddish, and the other CS/OD/TOB/PPY@PDA hydrogels showed the same pale yellow color as negative control PBS. The above results indicate that the CS/OD/TOB/PPY@PDA9 hydrogel has good hemocompatibility.

Furthermore, the cytocompatibility of CS/OD/TOB/PPY@PDA hydrogels was tested. The results in Figure 3c showed that despite a CS/OD/TOB/PPY@PDA hydrogel concentration as high as 20 mg/mL, the cell viability of all hydrogel groups is still higher than 88% of the tissue culture plate (TCP), indicating that the hydrogel has no toxic leachate. In addition, Figure 3d shows the results after CS/OD/TOB/PPY@PDA hydrogels were contacted with L929 cells for 24 h. Although the cell viability decreased to some extent with the incorporation of TOB and PPY@PDA, the cell viability of the QCS/OD/TOB/PPY@PDA12 hydrogel group was 67%, and the cell viability of the other hydrogel groups was still higher than 80%. The results of live/dead straining in each group were consistent with the quantitative results. Most cells were green and spindle-like in shape, while the CS/OD/TOB/PPY@PDA12 hydrogel group had more red dead cells (Figure 3e). All the above results indicate that when the content of PPY@PDA in the hydrogel is not higher than 12 mg/mL, the CS/OD/TOB/PPY@PDA hydrogel has good biocompatibility and can be used as a medical wound dressing.

***In Vitro* Drug Release.** Hydrogels with responsive drug release behavior have great advantages in the biomedical field.[58,59] The Schiff base-based hydrogels exhibit pH-dependent degradation behavior,[60] so the pH-dependent drug release behavior of QCS/OD/TOB/PPY@PDA hydrogels was evaluated in a physiological microenvironment (PBS, pH = 7.4) and a slightly acidic microenvironment (PBS, pH = 5.5), respectively. The results in Figure 4a show that in the slightly acidic microenvironment, the TOB in the hydrogel is rapidly released, and 45% of the total drug is released in only 6 h, while the hydrogel in the physiological microenvironment at this time only released 18% TOB. Even if TOB in the physiological microenvironment was continuously released for 9 days, its drug release amount was only 31%, and the drug release in the slightly acidic microenvironment reached 55%. The reason for the slow release of TOB in QCS/OD/TOB/PPY@PDA hydrogels is the cross-linking reaction of TOB with OD in the hydrogels. In addition, the QCS/OD/TOB

https://doi.org/10.1021/acsnano.2c05557
ACS Nano 2022, 16, 13022−13036

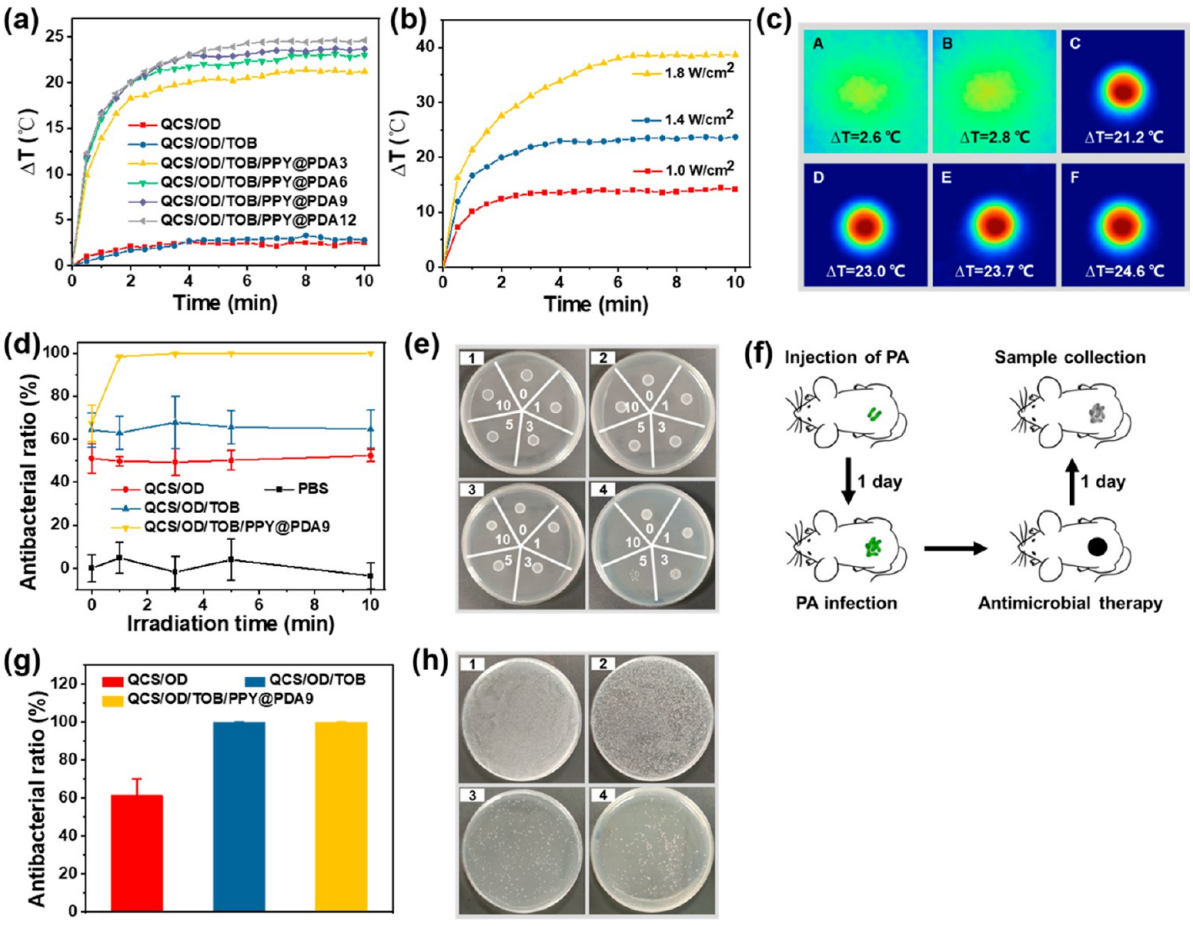

Figure 6. (a) ΔT−time curves of QCS/OD/TOB/PPY@PDA hydrogels under a light intensity of 1.4 W/cm^2. (b) ΔT−time curves of the QCS/OD/TOB/PPY@PDA9 hydrogel under different light intensities. (c) Heat maps of QCS/OD/TOB/PPY@PDA hydrogels after 10 min of NIR 808 nm irradiation with a constant light intensity of 1.4 W/cm^2 (A for QCS/OD, B for QCS/OD/TOB, C for QCS/OD/TOB/PPY@PDA3, D for QCS/OD/TOB/PPY@PDA6, E for QCS/OD/TOB/PPY@PDA9, and F for QCS/OD/TOB/PPY@PDA12). (d) Antibacterial ratio−time curves for methicillin-resistant *Staphylococcus aureus* (MRSA) of QCS/OD/TOB/PPY@PDA hydrogels when they are irradiated with a NIR light intensity of 1.4 W/cm^2. (e) Photographs of surviving MRSA after irradiation in the near-infrared exposed to a light intensity of 1.4 W/cm^2. (f) Process of *in vivo* antibacterial experiments (1 for PBS, 2 for QCS/OD, 3 for QCS/OD/TOB, and 4 for QCS/OD/TOB/PPY@PDA9). (g) *In vivo* antibacterial activity of QCS/OD/TOB/PPY@PDA hydrogels for PA. (h) Photograph of agar plate counts of infected tissues treated under different experimental conditions (1 for PBS, 2 for QCS/OD, 3 for QCS/OD/TOB, and 4 for QCS/OD/TOB/PPY@PDA9).

hydrogel and QCS/OD/TOB/PPY@PDA9 hydrogel exhibited similar TOB release profiles in the same microenvironment, which indicates that the incorporation of PPY@PDA9 does not affect TOB release. All the above results indicate that TOB from QCS/OD/TOB/PPY@PDA hydrogels can be released slowly and the release rate can be adjusted by changing the pH value of the microenvironment.

TOB Releases Antibacterial Activity in Liquid Medium (Mueller-Hinton Broth [MHB] Environment). Bacteria produce acidic products such as carbonic acid and lactic acid during respiration and fermentation on growth, turning the surrounding environment into a slightly acidic microenvironment.[32,61] Therefore, bacterial growth can promote the degradation of QCS/OD/TOB/PPY@PDA hydrogels and the release of TOB (Figure 4b). TOB has an excellent bactericidal effect,[62] so QCS/OD/TOB/PPY@PDA hydrogels have the potential to deal with infected burns. It is worth mentioning that the QCS/OD/TOB/PPY@PDA hydrogels slowly released a small amount of TOB in the absence of a large number of bacteria, preventing the abuse of antibiotics. To evaluate the antibacterial activity of QCS/OD/TOB/PPY@PDA hydrogels in a liquid environment, we first immersed the optimized 0.5 mL QCS/OD/TOB/PPY@PDA9 hydrogel into 5 mL of 10^4, 10^5, 10^6, 10^7, and 10^8 CFU/mL PA, SA, and *Escherichia coli* (EC) suspensions, respectively. The results showed (Figure S4) that the QCS/OD/TOB/PPY@PDA9 hydrogel could kill all 5 mL of 10^8 CFU/mL PA, SA, and EC within 36 h, showing an excellent bactericidal effect. Subsequently, we immersed different 0.5 mL hydrogel samples into 5 mL of 10^7 CFU/mL PA, SA, and EC suspensions, respectively, to evaluate the antibacterial impact of each component of the hydrogel. The bacterial suspension without any hydrogel was used as the positive control, and the MHB aqueous solution was used as the negative control. The results are shown in Figure 4c−e. The PA, SA, and EC of the positive control and TOB-free QCS/OD hydrogel groups continued to grow over time, while the OD_{600} values of bacteria in other hydrogel groups were equal to those of MHB after 3 h of incubation and did not increase subsequently. This showed that TOB is the main antimicrobial component in this test. In addition, the hydrogels after 24 h of immersion in the bacterial suspension still has good mechanical properties

https://doi.org/10.1021/acsnano.2c05557
ACS Nano 2022, 16, 13022−13036

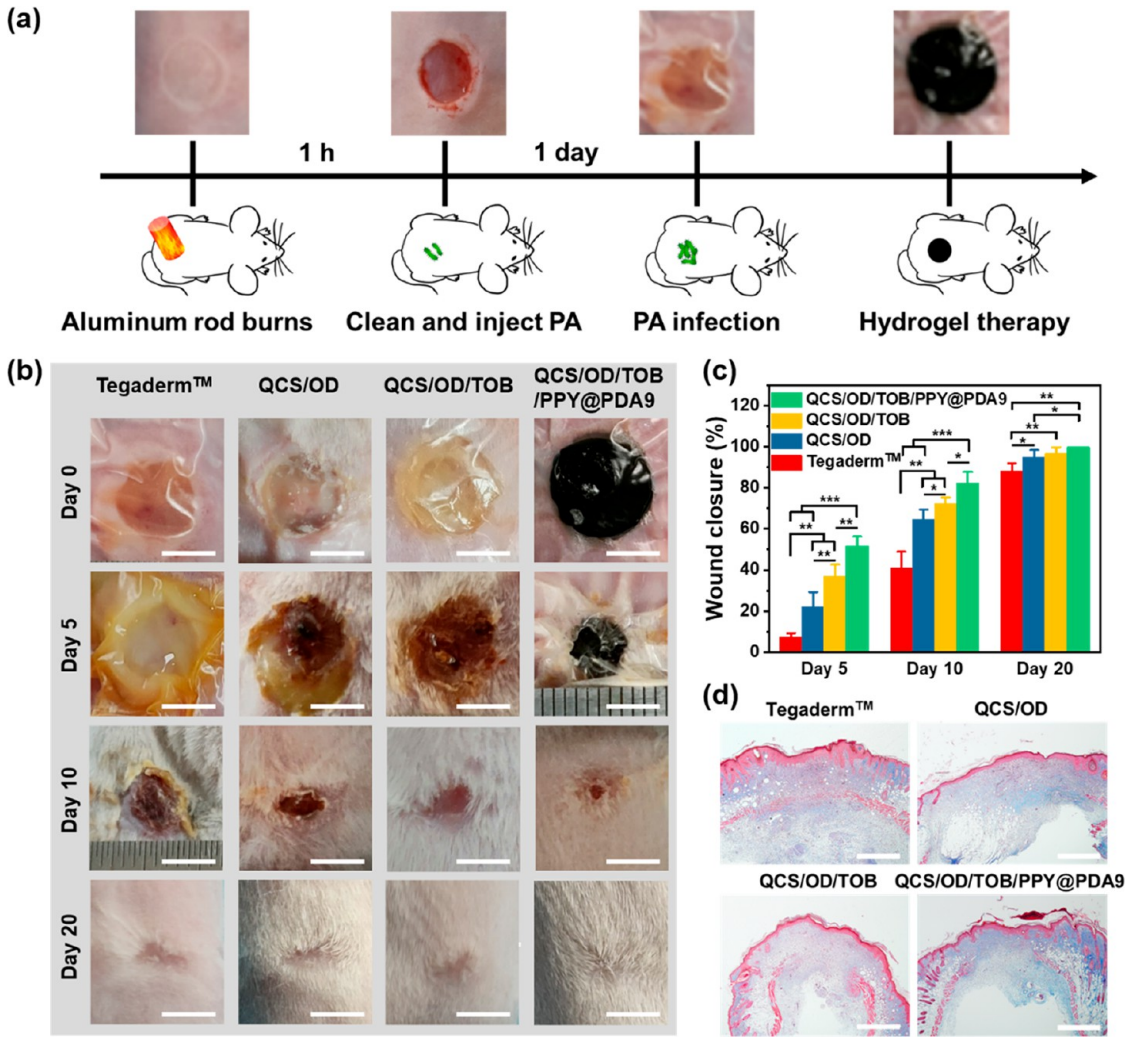

Figure 7. (a) Construction process of the PA-infected burn wound model. (b) Wound photographs after QCS/OD/TOB/PPY@PDA hydrogel treatment. Scale bar: 5 mm. (c) Wound contraction after QCS/OD/TOB/PPY@PDA hydrogel treatment. (d) Images of Masson's trichrome staining on day 10 after QCS/OD/TOB/PPY@PDA hydrogel treatment. Scale bar: 800 μm.

(Figure S5) without affecting its antibacterial properties. Therefore, we transferred the hydrogel that had completely killed 5 mL of 10^7 CFU/mL bacteria to another 5 mL of 10^7 CFU/mL bacterial suspension and tested the OD_{600} value of the bacterial suspension again after 24 h of incubation. Figure 4f,g show that both the QCS/OD/TOB hydrogel and the QCS/OD/TOB/PPY@PDA9 hydrogel that had completely killed 5 mL of 10^7 CFU/mL bacteria can again completely kill all 5 mL of 10^7 CFU/mL PA, SA, and EC. All the above results indicated that the QCS/OD/TOB/PPY@PDA hydrogel has an excellent antibacterial ability by releasing TOB in a liquid environment, which is a huge advantage in dealing with infected wounds.

TOB Releases Antibacterial Activity in Solid Medium (Agar Diffusion Test). To explore whether the QCS/OD/TOB/PPY@PDA hydrogel can sustainably kill bacteria growing in a solid medium, that is, whether TOB can be released sustainably in a solid medium, we evaluated the antibacterial activity of the QCS/OD/TOB/PPY@PDA hydrogel in a solid environment by agar diffusion experiments. The results in Figure 5a–c show that except for the QCS/OD hydrogel without TOB, the QCS/OD/TOB hydrogel and the QCS/OD/TOB/PPY@PDA9 hydrogel showed good antibacterial activity for PA, SA, and EC. On day 1, the inhibition zone diameters of both hydrogels for SA and EC were more than 20 mm, while the inhibition zone diameter for PA was as high as 34 mm. Although the antibacterial time of the QCS/OD/TOB/PPY@PDA9 hydrogel for EC was only 7 days, it showed an antibacterial time of up to 11 days for PA and SA, which commonly infect burn wounds. Wound infection usually occurs in the early stage of wound healing, and even for wounds with delayed healing, the inflammatory period usually does not exceed 10 days,[5,40,63] so the QCS/OD/TOB/PPY@PDA9 hydrogel with an antibacterial time of 11 days in agar plates has the ability to cope with slowly healing infected burn wounds. Figure 5d–f show the inhibition zone diameter changes of different bacteria at different times. In addition, although QCS/OD hydrogels do not possess release antibacterial activity, they still exhibited good contact antibacterial activity (Figure S6). The above results indicate that the QCS/OD/TOB/PPY@PDA hydrogel also has excellent antibacterial activity in a solid environment and has great potential for treating infected burn wounds.

Photothermal and NIR Irradiation Assisted Bactericidal Activity of Drug-Resistant Bacteria. Materials with NIR-responsive photothermal properties also have the ability

https://doi.org/10.1021/acsnano.2c05557
ACS Nano 2022, 16, 13022–13036

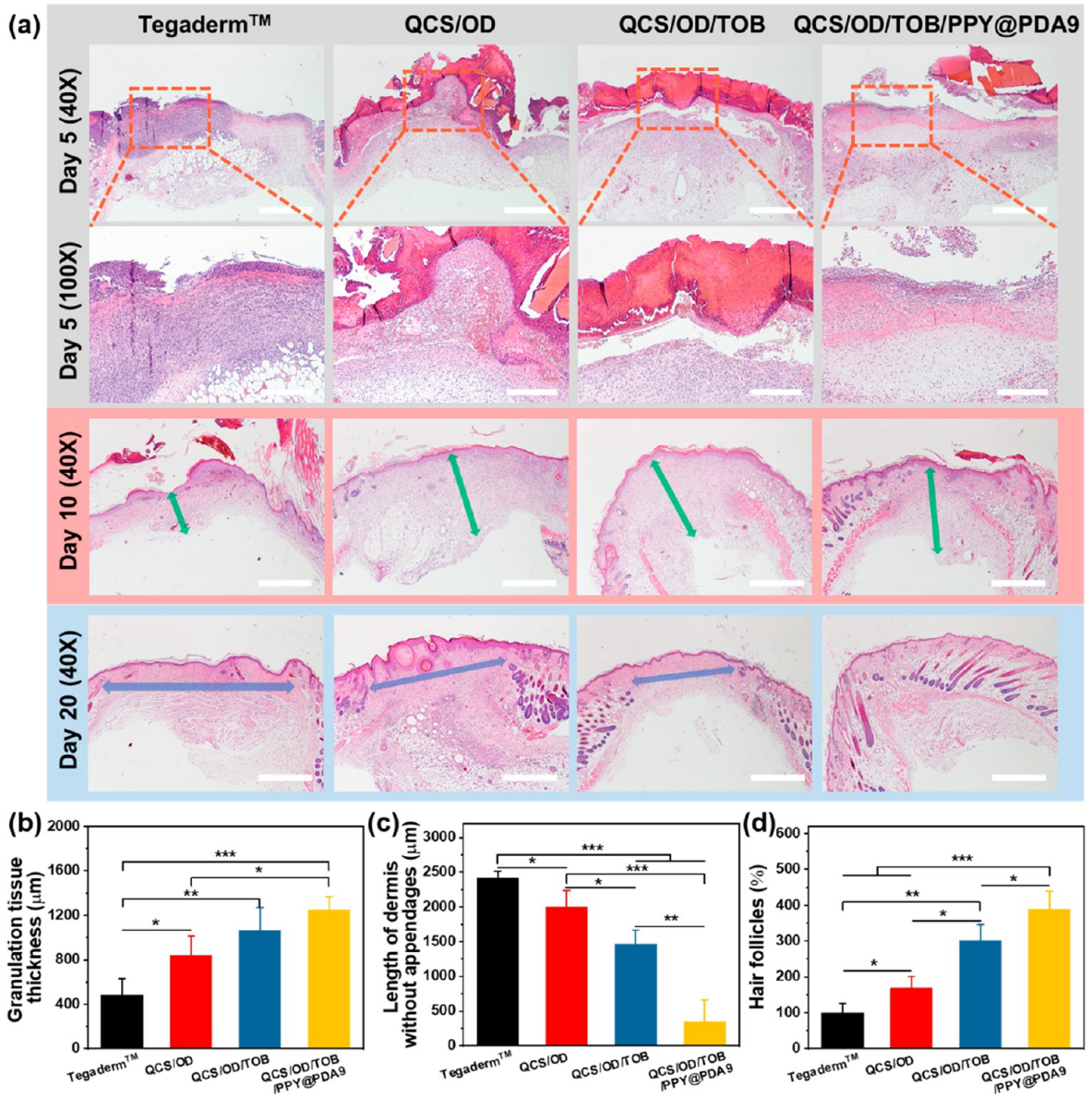

Figure 8. (a) Histomorphological analysis of wound regeneration after QCS/OD/TOB/PPY@PDA hydrogel treatment (green arrows mark the granulation tissue; blue arrows mark the dermis without appendages). Scale bar: 800 μm for 40× and 300 μm for 100×. (b) Quantitative data of granulation tissue thickness on day 10. (c) Quantitative data of the length of dermis without appendages on day 20. (d) Hair follicles of different groups on day 20. The hair follicle data on day 20 in the Tegaderm dressing group were taken as 100%.

to deal with drug-resistant bacteria.[64,65] First, we evaluated the photothermal properties of the QCS/OD/TOB/PPY@PDA hydrogel by ΔT−NIR irradiation time curves. Figure 6a shows that the QCS/OD hydrogel and QCS/OD/TOB hydrogel without the addition of PPY@PDA showed little change after 10 min of NIR irradiation and only increased by 2.5 °C. After adding PPY@PDA, the photothermal effect of the QCS/OD/TOB/PPY@PDA hydrogel was rapidly improved, and the temperature of the QCS/OD/TOB/PPY@PDA3 hydrogel increased by 21 °C after 10 min of NIR irradiation. Correspondingly, the ΔT of the hydrogels after 10 min of NIR irradiation continued to increase with increasing PPY@PDA content. This indicates that PPY@PDA provides good photothermal properties for QCS/OD/TOB/PPY@PDA hydrogels. In addition, Figure 6b shows that the QCS/OD/TOB/PPY@PDA9 hydrogel has tunable photothermal properties, and the ΔT of QCS/OD/TOB/PPY@PDA9 hydrogels increased or decreased with increasing or decreasing NIR intensity. Figure 6c and Figure S7 show the heat map of the hydrogel after 10 min of NIR irradiation. The core region in the heat map has a large temperature difference from the surrounding area, which facilitates local heat treatment without damaging the surrounding tissue. The above results indicate that the QCS/OD/TOB/PPY@PDA hydrogel has excellent tunable photothermal properties and can be used to eliminate drug-resistant bacteria. Finally, the photothermal antibacterial efficiency of QCS/OD/TOB/PPY@PDA hydrogels was evaluated by PBS as a control group. Figure 6d shows that the sterilization ratio of QCS/OD hydrogels and QCS/OD/TOB hydrogels with poor photothermal properties did not increase with increasing NIR irradiation time, but had 50% and 65% sterilization ratios. This is the result of the QCS in the hydrogel being in contact with the bacteria for 10 min, and the sterilization ratio of the QCS/OD/TOB hydrogel was slightly

https://doi.org/10.1021/acsnano.2c05557
ACS Nano 2022, 16, 13022−13036

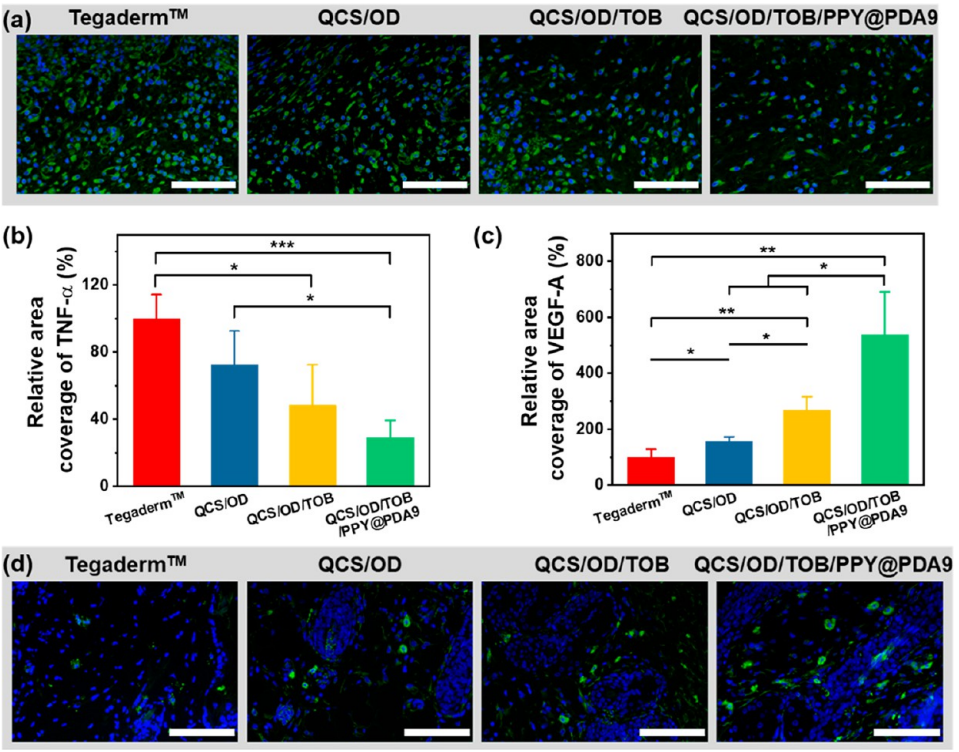

Figure 9. Images of immunofluorescence labeling of the regenerated tissue of wounds stained with (a) TNF-α on day 5 and (d) VEGF-A on day 10. Scale bar: 100 μm. (b) Relative area percentage of TNF-α and (c) quantitative analysis of relative area percentage of VEGF-A. Data for TNF-α for the Tegaderm dressing group on day 5 and VEGF-A on day 10 were taken as 100%, respectively.

higher than that of the QCS/OD hydrogel because of the effect of TOB. The QCS/OD/TOB/PPY@PDA9 hydrogel with good photothermal effect achieved a sterilization ratio of 98% after only 1 min of NIR irradiation. After 10 min of irradiation, the sterilization ratio reached 100%. All the above results indicate that the QCS/OD/TOB/PPY@PDA hydrogel has good NIR irradiation-assisted antibacterial properties.

***In Vivo* Antibacterial Activity.** Having good antibacterial ability *in vivo* is the key to dealing with infected wounds.[42] The *in vivo* antibacterial model was consistent with the burn wound repair model, the PA-infected burn wound model was used to evaluate the *in vivo* antibacterial ability of QCS/OD/TOB/PPY@PDA hydrogels, and PBS was used as a control. As shown in Figure 6f, the modeling was successful and the samples were collected and counted after 1 day of hydrogel treatment. Figure 6g shows that the bactericidal ratio of the QCS/OD hydrogel with the polycation is 61%. The sterilization ratio of the QCS/OD/TOB hydrogel and QCS/OD/TOB/PPY@PDA9 hydrogel loaded with TOB was as high as 99.97%. Figure 6h is a photograph of agar plate counts of infected tissues treated under different experimental conditions, consistent with the quantitative results. The above results indicate that the QCS/OD/TOB/PPY@PDA9 hydrogel possesses excellent antibacterial activity *in vivo* and has great potential in promoting the healing of infected burn wounds.

***In Vivo* Wound Healing in PA-Infected Burn Wound Model.** Burns are a very common health problem, and burn wounds are susceptible to PA infection.[66] Therefore, the PA-infected burn wound model was selected to evaluate the ability of the QCS/OD/TOB/PPY@PDA hydrogel to promote burn wound healing. The model was constructed as shown in Figure 7a. First, a circular scalded wound was created on the back of the mouse through an aluminum rod heated by boiling water. After 1 h, the wound was debrided and PA was injected. After 1 day, the burn wound was successfully infected with PA, and the QCS/OD/TOB/PPY@PDA hydrogel was used to treat the wound at this time. A commercial film dressing, Tegaderm, was used as a control. Results after 5 days of treatment (Figure 7b,c) showed that the wound contraction of Tegaderm was only 7% due to severe wound infection. The wound contraction of the QCS/OD group with a good bactericidal effect reached 22%. The wound contraction of the antibiotic smart release QCS/OD/TOB group was further improved to 37%. However, the wound contraction of the QCS/OD/TOB/PPY@PDA9 group with good electrical conductivity was as high as 52%. The wounds in each group further contracted as the treatment time increased. After 10 days of treatment, wounds in the Tegaderm and QCS/OD groups remained mildly infected, with wound contractions of 41% and 65%, respectively. In contrast, the wound contraction of the QCS/OD/TOB group and the QCS/OD/TOB/PPY@PDA9 group was 73% and 82%, respectively. After 20 days of treatment, the wounds in the QCS/OD/TOB/PPY@PDA9 group contracted completely, while the wound contraction in the Tegaderm group was only 88%. The above results indicate that the QCS/OD/TOB/PPY@PDA9 hydrogel can accelerate wound contraction and provide a basis for wound healing. In addition, wound healing is accompanied by the metabolism of collagen, so the deposition of collagen also reflects the process of wound healing. Figure 7d shows the results of Masson's trichrome staining of wounds after 10 days of treatment. The Tegaderm, QCS/OD, and QCS/OD/TOB groups all had only a small amount of collagen deposition, while the QCS/OD/TOB/PPY@PDA9 group showed a higher amount of collagen deposition, which was significantly higher than the other three

https://doi.org/10.1021/acsnano.2c05557
ACS Nano 2022, 16, 13022−13036

groups. This indicates that QCS/OD/TOB/PPY@PDA9 can promote collagen deposition, which is beneficial to wound healing. All the above results indicate that QCS/OD/TOB/PPY@PDA9 has an excellent ability to promote the healing of infected burn wounds.

Histological and Immunochemical Analysis. Histological and immunochemical analysis by hematoxylin−eosin (HE) staining is an important means to assess the progress of wound healing and the quality of regenerated skin.[67] In the early stage of wound healing, fibroblasts and inflammatory cells are recruited at the wound site, showing a mild acute inflammatory response.[22] However, the results in Figure 8a showed that after 5 days of treatment the wounds in the Tegaderm group exhibited severe inflammatory responses due to severe PA infection, which would prolong the inflammatory phase of the repair process, hinder the wound healing, and possibly even be life-threatening. After treatment with the TOB smart release hydrogel, the inflammatory response was greatly alleviated, showing a mild inflammatory response. When the treatment time was extended to 10 days, the wounds in the Tegaderm group finally ended the inflammatory phase and began to enter the proliferative phase. At this time, the wounds of other groups had formed thicker granulation tissue.

Granulation tissue fills wound voids and provides the basis for angiogenesis, so thick granulation tissue is a favorable factor for wound healing. Figure 8b showed that the thickness of the granulation tissue in the Tegaderm group was only 481 μm, while the thickness of the granulation tissue in the QCS/OD group reached 840 μm. In addition, the thickness of the granulation tissue in the QCS/OD group, the QCS/OD/TOB group, and the QCS/OD/TOB/PPY@PDA9 group increased sequentially, and the thickness of the granulation tissue in the QCS/OD/TOB/PPY@PDA9 group was as high as 1249 μm. After 20 days of treatment, the wounds in the QCS/OD/TOB/PPY@PDA9 group were almost completely remodeled, with a large number of hair follicles growing and showing neatly arranged connective tissue. At this time, the wounds in the Tegaderm group still showed a length of dermis without appendages, 2414 μm in length (Figure 8c). Although QCS/OD and QCS/OD/TOB had a favorable promoting effect on wound healing, the length of the dermis without appendages was still as long as 2001 and 1466 μm. However, the length of the dermis without appendages in the QCS/OD/TOB/PPY@PDA9 group was only 352 μm, which was significantly lower than that in the other groups ($P < 0.01$). In addition, Figure 8d shows that the Tegaderm group only had a small number of hair follicles, and the QCS/OD/TOB/PPY@PDA9 group had the most hair follicles, which was significantly higher than the other groups ($P < 0.05$). All the above results indicated that the QCS/OD/TOB/PPY@PDA9 hydrogel can fight infection and alleviate the inflammatory response while promoting wound closure and granulation tissue generation, which is an excellent choice for the treatment of burns.

Tumor Necrosis Factor-α (TNF-α) and Vascular Endothelial Growth Factor-A (VEGF-A) Expression. Infected wounds are often accompanied by severe inflammatory cell infiltration, and the level of inflammation in wounds is quantitatively assessed by the TNF-α expression.[68] Consistent with the results of HE staining (Figure 9a,b), at the early wound healing (day 5), the inflammation levels were reduced to varying degrees in all hydrogel groups compared to the Tegaderm group. The QCS/OD/TOB/PPY@PDA9 group showed the lowest TNF-α expression, which was significantly lower than the Tegaderm and QCS/OD groups ($P < 0.05$). This is because the QCS/OD hydrogel has antibacterial ability, which can appropriately relieve wound infection. The QCS/OD/TOB/PPY@PDA9 hydrogel has excellent TOB intelligent release antibacterial ability, which can effectively deal with PA infection, making the wound microenvironment maintain appropriate levels of inflammation.

In addition, neovascularization is an important way to transport growth factors and nutrients to the wound site, so the number of neovascularizations greatly reflects the efficiency of wound healing.[67] The level of neovascularization in the wound was quantitatively assessed by the VEGF-A expression during the proliferative phase (day 10).[69] Figure 9c,d show that the QCS/OD/TOB/PPY@PDA9 group had a high expression of VEGF-A, 5-fold that of the Tegaderm group and significantly higher than the other groups ($P < 0.05$). This indicates that the QCS/OD/TOB/PPY@PDA9 hydrogel can promote angiogenesis.

***In Vivo* Host Response.** Biomaterials in direct contact with biological tissues should have good histocompatibility. Evaluation of the *in vivo* biocompatibility of the hydrogels was performed by subcutaneously implanting QCS/OD/TOB/PPY@PDA hydrogels in rats and observing the host response. Figure S8 shows that after 7 days of subcutaneous implantation in rats all groups showed a mild inflammatory response and thin fibrous connective tissue. After 28 days of subcutaneous implantation in rats, the inflammatory response receded, and the fibrous connective tissue was further thinned. The above results indicate that the QCS/OD/TOB/PPY@PDA hydrogel has good histocompatibility.

CONCLUSIONS

We prepared a series of self-healing hydrogels with bacterial growth-induced TOB smart release. The hydrogel has good electrical conductivity and excellent antioxidant activity as well as good biocompatibility. Importantly, the QCS/OD/TOB/PPY@PDA hydrogels showed intelligent release of TOB and exhibited excellent antibacterial ability. The long-term release of TOB on agar plates indicated its ability to cope with the slow wound healing of infected burn wounds. In addition, the photothermal properties conferred by PPY@PDA and the polycation of QCS endow the hydrogel with a good ability to kill drug-resistant bacteria. The optimized QCS/OD/TOB/PPY@PDA9 hydrogel showed better wound contraction and collagen deposition than Tegaderm in the PA-infected burn wound model, and the QCS/OD/TOB/PPY@PDA9 hydrogel can effectively control the level of inflammation and promote angiogenesis. Therefore, the QCS/OD/TOB/PPY@PDA hydrogel has great advantages for repair of infected burn wounds.

EXPERIMENTAL SECTION

Materials. Chitosan, dopamine hydrochloride, and GTMAC were purchased from J&K. Pyrrole and dextran were purchased from Macklin. APS, SP, and TOB were purchased from Aladdin.

Synthesis of QCS and OD. The synthesis procedure of QCS and OD was in accord with previously reported methods,[22,32] which is detailed in the Supporting Information.

Synthesis of PPY@PDA NWs. The synthesis procedure of PPY@PDA was performed based on the previously reported method with a few modifications.[42] Briefly, 0.48 mL of pyrrole monomer and 0.2 g of dopamine hydrochloride (pyrrole:dopamine = 6:1) were dissolved in 100 mL of Tris solution (pH = 8.5, 0.01 M) and cooled in an ice water bath. Two grams of ammonium persulfate dissolved in 20 mL of

https://doi.org/10.1021/acsnano.2c05557
ACS Nano 2022, 16, 13022−13036

Tris solution was added dropwise to the above solution with vigorous stirring at low temperature and then transferred to a refrigerator at 8 °C with vigorous stirring for 18 h. After the reaction was completed, the precipitate was washed several times with deionized water and collected by centrifugation. Finally, the washed precipitate was lyophilized to obtain PPY@PDA powder.

Preparation of TOB Smart Release Hydrogel (QCS/OD/TOB/PPY@PDA). Briefly, QCS was first dissolved in deionized water to obtain the QCS solution, and then PPY@PDA was added to the QCS solution and dispersed under ultrasonication for 1 h to obtain the QCS/PPY@PDA solution. In addition, OD and TOB were dissolved in deionized water to obtain an OD solution and a TOB solution, respectively. The QCS solution, QCS/PPY@PDA solution, OD solution, and TOB solution were mixed in different proportions under vigorous shaking to obtain a TOB smart release hydrogel in a short time. The prepared hydrogels were named QCS/OD/TOB/PPY@PDA*n*, where *n* indicates the concentration of PPY@PDA in the hydrogel as mg/mL. In addition, the hydrogel without PPY@PDA was named QCS/OD/TOB, and the hydrogel containing neither PPY@PDA nor TOB was named QCS/OD. The hydrogel components in detail are shown in Table 1.

Table 1. Concentration (mg/mL) of Each Component in the Hydrogel

hydrogel	QCS	OD	TOB	PPY@PDA
QCS/OD	20	35	0	0
QCS/OD/TOB	20	35	13	0
QCS/OD/TOB/PPY@PDA3	20	35	13	3
QCS/OD/TOB/PPY@PDA6	20	35	13	6
QCS/OD/TOB/PPY@PDA9	20	35	13	9
QCS/OD/TOB/PPY@PDA12	20	35	13	12

Characterizations. TEM was used to confirm the physical properties of the PPY@PDA NWs. The XPS analysis, rheological measurements, degradation test, conductivity test, and antioxidant activity[70] test were used to confirm the physical and chemical properties of QCS/OD/TOB/PPY@PDA hydrogels, which are detailed in the Supporting Information.

Biocompatibility. The biocompatibility of QCS/OD/TOB/PPY@PDA hydrogels was evaluated by hemocompatibility test and cytocompatibility test,[71] which are detailed in the Supporting Information.

***In Vitro* Drug Release.** *In vitro* drug release by an *o*-phthalaldehyde derivatization method for the determination of TOB in the release solution,[72] which is detailed in the Supporting Information.

TOB Releases Antibacterial Activity. The TOB release of antibacterial activity of QCS/OD/TOB/PPY@PDA hydrogels was evaluated using Gram-positive bacteria SA, Gram-negative bacteria EC, and Gram-negative PA closely related to burns. The TOB release of antibacterial activity of the hydrogels in liquid and solid media was evaluated by the MHB diffusion test and agar diffusion test, respectively.

For the MHB diffusion test, 0.5 mL of QCS/OD/TOB/PPY@PDA9 hydrogel was first added to 5 mL of 10^4, 10^5, 10^6, 10^7, and 10^8 CFU/mL bacterial suspension, respectively, to preliminarily judge the released antibacterial effect of the QCS/OD/TOB/PPY@PDA hydrogel. Then 0.5 mL of QCS/OD, QCS/OD/TOB, and QCS/OD/TOB/PPY@PDA*n* hydrogels were added to 5 mL of a 10^7 CFU/mL bacterial suspension, respectively. Subsequently, the bacterial suspension was transferred to a shaker at 37 °C for aerobic cultivation. At predetermined time points, 100 μL of a bacterial suspension was taken and the absorbance was read at 600 nm with a microplate reader. MHB and bacterial suspensions without hydrogel were used as controls. In addition, 0.5 mL of QCS/OD/TOB and QCS/OD/TOB/PPY@PDA9 hydrogels were immersed in 5 mL of a 10^7 CFU/mL bacterial suspension for 24 h and then replaced with another 5 mL of 10^7 CFU/mL bacterial suspension. After culturing for 24 h, the absorbance was read again with a microplate reader, and this cycle was performed to evaluate the effective sterilization batch of 0.5 mL of the QCS/OD/TOB/PPY@PDA hydrogel.

For the agar diffusion test,[73] the agar plates were inoculated with 100 μL of bacterial suspension (10^8 CFU/mL) by spreading. Cylindrical hydrogels with a diameter of 4 mm and a height of 1 mm were then placed on the inoculated agar plates, and the inhibition zone around each sample was measured after incubation in a constant-temperature incubator at 37 °C for 24 h. The samples were then transferred to a freshly inoculated agar plate, and the diameter of the inhibition zone was measured again after 24 h of incubation. The above procedure was repeated until no zone of inhibition is observed on the freshly inoculated agar plate. The QCS/OD hydrogel without TOB was used as a control.

Photothermal and NIR Irradiation Assisted Bactericidal Activity of Drug-Resistant Bacteria. The photothermal performance and NIR irradiation assisted bactericidal activity of drug-resistant bacteria of QCS/OD/TOB/PPY@PDA hydrogels were evaluated according to previously reported methods,[43] which is detailed in the Supporting Information.

***In Vivo* Antibacterial Activity.** The *in vivo* antibacterial activity of QCS/OD/TOB/PPY@PDA hydrogels was evaluated by a PA-infected burn wound model. Samples were collected from the wound site after 1 day of treatment. Any bacterial survivors in the samples were resuspended with sterilized PBS. Then 10 μL of the above resuspension was added to agar plates, and colony-forming units on the agar plates were counted after incubation at 37 °C for 18 to 24 h. The antibacterial efficiency was expressed as an antibacterial ratio using the following equation: antibacterial ratio (%) = $(C_c - C_h)/C_c \times 100\%$. C_c and C_h represent the count of bacteria in the control group and the count of bacteria in the hydrogel group, respectively. The modeling details are available in the Wound Healing in Vivo in a PA-Infected Burn Wound Model section.

Wound Healing *in Vivo* in a PA-Infected Burn Wound Model. A PA-infected burn wound model was established on the back of female Kunming mice (30−35 g) by previously reported methods with some modifications.[74] First, after the mice were anesthetized, the dorsal area was shaved. Then, an aluminum metal rod with a length of 6.5 cm and a diameter of 7 mm was heated in boiling water for 10 min, and then the water on the surface of the metal rod was immediately wiped off with gauze and directly contacted with the mouse skin for 2 min. The pressure on the mouse's back was provided only by the metal rod, and no other external force was applied. The pressure of the metal rod on the mouse skin was 1778 kPa. One hour after the deep second-degree burn model was established, a biopsy punch of the same diameter was used to remove the burned dead tissue, which mimics the clinical practice of removing severely burned skin. Subsequently, 10 μL of 10^8 CFU/mL PA was added to the wound. After 1 day of feeding, the wounds were infected with PA, and the PA-infected burn wound model was successfully constructed. At this time, different dressings are used to treat the infected wound. Wound dressings include transparent film dressing frame style (3M Health Care, USA), QCS/OD, QCS/OD/TOB, and QCS/OD/TOB/PPY@PDA9 hydrogels. The wound area was photographed after 5, 10, and 20 days of treatment, and wound contraction was measured and calculated by ImageJ software. Wound contraction (%) = $(A_0 - A_n)/A_0 \times 100\%$, where A_0 and A_n represent the wound area on day 0 and day *n*, respectively.

Histological and Immunochemical Analysis. The samples were immunohistochemistry stained with TNF-α and VEGF-A by a standard protocol to assess inflammation and angiogenesis, which is detailed in the Supporting Information.

ASSOCIATED CONTENT

Supporting Information

The Supporting Information is available free of charge at https://pubs.acs.org/doi/10.1021/acsnano.2c05557.

Detailed preparation and characterization methods of hydrogels and their components, the number of amino

https://doi.org/10.1021/acsnano.2c05557
ACS Nano 2022, 16, 13022−13036

or aldehyde groups of each component of hydrogels, XPS N 1s spectrum and FT-IR spectrum of PPY@PDA, XPS N 1s spectrum of hydrogels, rheological properties of hydrogels, bacterial growth curves after hydrogel treatment, rheological behavior of hydrogels after 24 h of immersion in bacterial suspensions, HE staining results of hydrogels (PDF)

AUTHOR INFORMATION

Corresponding Author

Baolin Guo − *State Key Laboratory for Mechanical Behavior of Materials and Frontier Institute of Science and Technology, Xi'an Jiaotong University, Xi'an 710049, China; Key Laboratory of Shaanxi Province for Craniofacial Precision Medicine Research, College of Stomatology, Xi'an Jiaotong University, Xi'an 710049, China;* orcid.org/0000-0001-6756-1441; Phone: +86-29-83395043; Email: baoling@mail.xjtu.edu.cn; Fax: +86-29-83395131

Authors

Ying Huang − *State Key Laboratory for Mechanical Behavior of Materials and Frontier Institute of Science and Technology, Xi'an Jiaotong University, Xi'an 710049, China*

Lei Mu − *State Key Laboratory for Mechanical Behavior of Materials and Frontier Institute of Science and Technology, Xi'an Jiaotong University, Xi'an 710049, China*

Xin Zhao − *State Key Laboratory for Mechanical Behavior of Materials and Frontier Institute of Science and Technology, Xi'an Jiaotong University, Xi'an 710049, China*

Yong Han − *State Key Laboratory for Mechanical Behavior of Materials and Frontier Institute of Science and Technology, Xi'an Jiaotong University, Xi'an 710049, China;* orcid.org/0000-0002-4741-9058

Complete contact information is available at: https://pubs.acs.org/10.1021/acsnano.2c05557

Notes

The authors declare no competing financial interest.

ACKNOWLEDGMENTS

This work was jointly supported by the National Natural Science Foundation of China (grant number 51973172), the Natural Science Foundation of Shaanxi Province (No. 2020JC-03), State Key Laboratory for Mechanical Behavior of Materials, and the World-Class Universities (Disciplines) and the Characteristic Development Guidance Funds for the Central Universities. We also thank Instrument Analysis Center of Xi'an Jiaotong University for their assistance with XPS analysis.

REFERENCES

(1) Stoica, A. E.; Chircov, C.; Grumezescu, A. M. Hydrogel Dressings for the Treatment of Burn Wounds: An Up-to-Date Overview. *Materials* **2020**, *13* (12), 2853.

(2) Banerjee, J.; Seetharaman, S.; Wrice, N. L.; Christy, R. J.; Natesan, S. Delivery of Silver Sulfadiazine and Adipose Derived Stem Cells Using Fibrin Hydrogel Improves Infected Burn Wound Regeneration. *PLoS One* **2019**, *14* (6), No. e0217965.

(3) Stubbe, B.; Mignon, A.; Declercq, H.; Van Vlierberghe, S.; Dubruel, P. Development of Gelatin-Alginate Hydrogels for Burn Wound Treatment. *Macromol. Biosci.* **2019**, *19* (8), 1900123.

(4) Huang, W. J.; Wang, Y. X.; Huang, Z. Q.; Wang, X. L.; Chen, L. Y.; Zhang, Y.; Zhang, L. N. On-Demand Dissolvable Self-Healing Hydrogel Based on Carboxymethyl Chitosan and Cellulose Nanocrystal for Deep Partial Thickness Burn Wound Healing. *ACS Appl. Mater. Interfaces* **2018**, *10* (48), 41076−41088.

(5) Huang, Y.; Bai, L.; Yang, Y. T.; Yin, Z. H.; Guo, B. L. Biodegradable Gelatin/Silver Nanoparticle Composite Cryogel with Excellent Antibacterial and Antibiofilm Activity and Hemostasis for *Pseudomonas aeruginosa*-Infected Burn Wound Healing. *J. Colloid Interface Sci.* **2022**, *608*, 2278−2289.

(6) Oryan, A.; Jalili, M.; Kamali, A.; Nikahval, B. The Concurrent Use of Probiotic Microorganism and Collagen Hydrogel/Scaffold Enhances Burn Wound Healing: An *in Vivo* Evaluation. *Burns* **2018**, *44* (7), 1775−1786.

(7) Mai, B. J.; Jia, M. Q.; Liu, S. P.; Sheng, Z. H.; Li, M.; Gao, Y. R.; Wang, X. B.; Liu, Q. H.; Wang, P. Smart Hydrogel-Based DVDMS/bFGF Nanohybrids for Antibacterial Phototherapy with Multiple Damaging Sites and Accelerated Wound Healing. *ACS Appl. Mater. Interfaces* **2020**, *12* (9), 10156−10169.

(8) Li, Z. Y.; Zhou, F.; Li, Z. Y.; Lin, S. Y.; Chen, L.; Liu, L. X.; Chen, Y. M. Hydrogel Cross-Linked with Dynamic Covalent Bonding and Micellization for Promoting Burn Wound Healing. *ACS Appl. Mater. Interfaces* **2018**, *10* (30), 25194−25202.

(9) Dong, Y. X.; Cui, M. H.; Qu, J.; Wang, X. C.; Kwon, S. H.; Barrera, J.; Elvassore, N.; Gurtner, G. C. Conformable Hyaluronic Acid Hydrogel Delivers Adipose-Derived Stem Cells and Promotes Regeneration of Burn Injury. *Acta Biomater.* **2020**, *108*, 56−66.

(10) Chouhan, D.; Lohe, T. U.; Samudrala, P. K.; Mandal, B. B. *In Situ* Forming Injectable Silk Fibroin Hydrogel Promotes Skin Regeneration in Full Thickness Burn Wounds. *Adv. Healthcare Mater.* **2018**, *7* (24), 1801092.

(11) Shi, Y. F.; Zhang, H. J.; Zhang, X.; Chen, Z.; Zhao, D.; Ma, J. A Comparative Study of Two Porous Sponge Scaffolds Prepared by Collagen Derived from Porcine Skin and Fish Scales as Burn Wound Dressings in a Rabbit Model. *Regener. Biomater.* **2020**, *7* (1), 63−70.

(12) Li, J.; Ghatak, S.; El Masry, M. S.; Das, A.; Liu, Y.; Roy, S.; Lee, R. J.; Sen, C. K. Topical Lyophilized Targeted Lipid Nanoparticles in the Restoration of Skin Barrier Function Following Burn Wound. *Mol. Ther.* **2018**, *26* (9), 2178−2188.

(13) Bayat, S.; Amiri, N.; Pishavar, E.; Kalalinia, F.; Movaffagh, J.; Hahsemi, M. Bromelain-Loaded Chitosan Nanofibers Prepared by Electrospinning Method for Burn Wound Healing in Animal Models. *Life Sci.* **2019**, *229*, 57−66.

(14) Zeng, Q. K.; Qi, X. L.; Shi, G. Y.; Zhang, M.; Haick, H. Wound Dressing: From Nanomaterials to Diagnostic Dressings and Healing Evaluations. *ACS Nano* **2022**, *16* (2), 1708−1733.

(15) Hu, J. J.; Yang, L.; Cheng, X. J.; Li, Y. W.; Cheng, Y. Y. Aminoglycoside-Based Biomaterials: From Material Design to Antibacterial and Gene Delivery Applications. *Adv. Funct. Mater.* **2021**, *31* (36), 2103718.

(16) Ma, Q.; Wang, Y. X.; Jia, J.; Xiang, Y. H. Colorimetric Aptasensors for Determination of Tobramycin in Milk and Chicken Eggs Based on DNA and Gold Nanoparticles. *Food Chem.* **2018**, *249*, 98−103.

(17) Cheng, X. J.; Chen, H. Y.; Yang, F.; Hong, J. X.; Cheng, Y. Y.; Hu, J. J. All-Small-Molecule Supramolecular Hydrogels Assembled from Guanosine 5′-Monophosphate Disodium Salt and Tobramycin for the Treatment of Bacterial Keratitis. *Bioact. Mater.* **2022**, *16*, 293−300.

(18) Thorn, C. R.; Carvalho-Wodarz, C. D.; Horstmann, J. C.; Lehr, C. M.; Prestidge, C. A.; Thomas, N. Tobramycin Liquid Crystal Nanoparticles Eradicate Cystic Fibrosis-Related *Pseudomonas aeruginosa* Biofilms. *Small* **2021**, *17* (24), 2100531.

(19) Zhang, M. Y.; Chen, G.; Lei, M. H.; Lei, J. Q.; Li, D.; Zheng, H. A pH-Sensitive Oxidized-Dextran Based Double Drug-Loaded Hydrogel with High Antibacterial Properties. *Int. J. Biol. Macromol.* **2021**, *182*, 385−393.

(20) Schmidt, N. W.; Deshayes, S.; Hawker, S.; Blacker, A.; Kasko, A. M.; Wong, G. C. L. Engineering Persister-Specific Antibiotics with Synergistic Antimicrobial Functions. *ACS Nano* **2014**, *8* (9), 8786−8793.

(21) Liang, Y. Q.; Liang, Y. P.; Zhang, H. L.; Guo, B. L. Antibacterial Biomaterials for Skin Wound Dressing. *Asian J. Pharm. Sci.* **2022**, *17* (3), 353−384.
(22) Qu, J.; Zhao, X.; Liang, Y. P.; Zhang, T. L.; Ma, P. X.; Guo, B. L. Antibacterial Adhesive Injectable Hydrogels With Rapid Self-Healing, Extensibility and Compressibility as Wound Dressing for Joints Skin Wound Healing. *Biomaterials* **2018**, *183*, 185−199.
(23) Zhao, X.; Liang, Y. P.; Guo, B. L.; Yin, Z. H.; Zhu, D.; Han, Y. Injectable Dry Cryogels With Excellent Blood-Sucking Expansion and Blood Clotting to Cease Hemorrhage for Lethal Deep-Wounds, Coagulopathy and Tissue Regeneration. *Chem. Eng. J.* **2021**, *403*, 126329.
(24) Pok, S.; Vitale, F.; Eichmann, S. L.; Benavides, O. M.; Pasquali, M.; Jacot, J. G. Biocompatible Carbon Nanotube-Chitosan Scaffold Matching the Electrical Conductivity of the Heart. *ACS Nano* **2014**, *8* (10), 9822−9832.
(25) Zhao, X.; Guo, B. L.; Wu, H.; Liang, Y. P.; Ma, P. X. Injectable Antibacterial Conductive Nanocomposite Cryogels with Rapid Shape Recovery for Noncompressible Hemorrhage and Wound Healing. *Nat. Commun.* **2018**, *9*, 2784.
(26) Zhao, X.; Wu, H.; Guo, B. L.; Dong, R. N.; Qiu, Y. S.; Ma, P. X. Antibacterial Anti-Oxidant Electroactive Injectable Hydrogel as Self-Healing Wound Dressing with Hemostasis and Adhesiveness for Cutaneous Wound Healing. *Biomaterials* **2017**, *122*, 34−47.
(27) Huang, J. F.; Zhong, J.; Chen, G. P.; Lin, Z. T.; Deng, Y. Q.; Liu, Y. L.; Cao, P. Y.; Wang, B. W.; Wei, Y. T.; Wu, T. F.; Yuan, J.; Jiang, G. B. A Hydrogel-Based Hybrid Theranostic Contact Lens for Fungal Keratitis. *ACS Nano* **2016**, *10* (7), 6464−6473.
(28) Yu, R.; Li, M.; Li, Z. L.; Pan, G. Y.; Liang, Y. Q.; Guo, B. L. Supramolecular Thermo-Contracting Adhesive Hydrogel with Self-Removability Simultaneously Enhancing Noninvasive Wound Closure and MRSA-Infected Wound Healing. *Adv. Healthcare Mater.* **2022**, *11* (13), 2102749.
(29) Diamantstein, T.; Ruhl, H.; Vogt, W.; Bochert, G. Stimulation of B-Cells by Dextran Sulfate *in Vitro*. *Immunology* **1973**, *25* (4), 743−747.
(30) Yuan, F.; Sun, M. N.; Liu, Z. S.; Liu, H. Q.; Kong, W. J.; Wang, R.; Qian, F. Macropinocytic Dextran Facilitates KRAS-Targeted Delivery While Reducing Drug-Induced Tumor Immunity Depletion in Pancreatic Cancer. *Theranostics* **2022**, *12* (1), 1061−1073.
(31) Hu, J. J.; Zheng, Z.; Liu, C. X.; Hu, Q. Y.; Cai, X. P.; Xiao, J. R.; Cheng, Y. Y. A pH-Responsive Hydrogel with Potent Antibacterial Activity Against Both Aerobic and Anaerobic Pathogens. *Biomater. Sci.* **2019**, *7* (2), 581−584.
(32) Hu, J. J.; Quan, Y. C.; Lai, Y. P.; Zheng, Z.; Hu, Z. Q.; Wang, X. Y.; Dai, T. J.; Zhang, Q.; Cheng, Y. Y. A Smart Aminoglycoside Hydrogel with Tunable Gel Degradation, On-Demand drug release, and High Antibacterial Activity. *J. Controlled Release* **2017**, *247*, 145−152.
(33) Han, L.; Yan, L. W.; Wang, M. H.; Wang, K. F.; Fang, L. M.; Zhou, J.; Fang, J.; Ren, F. Z.; Lu, X. Transparent, Adhesive, and Conductive Hydrogel for Soft Bioelectronics Based on Light-Transmitting Polydopamine-Doped Polypyrrole Nanofibrils. *Chem. Mater.* **2018**, *30* (16), 5561−5572.
(34) Zhou, T.; Yan, L. W.; Xie, C. M.; Li, P. F.; Jiang, L. L.; Fang, J.; Zhao, C. C.; Ren, F. Z.; Wang, K. F.; Wang, Y. B.; Zhang, H. P.; Guo, T. L.; Lu, X. A Mussel-Inspired Persistent ROS-Scavenging, Electroactive, and Osteoinductive Scaffold Based on Electrochemical-Driven *in Situ* Nanoassembly. *Small* **2019**, *15* (25), 1805440.
(35) Song, C.; Zhang, X. Y.; Wang, L. Y.; Wen, F.; Xu, K. G.; Xiong, W. R.; Li, C. K.; Li, B. Y.; Wang, Q.; Xing, M. M. Q.; Qiu, X. Z. An Injectable Conductive Three-Dimensional Elastic Network by Tangled Surgical-Suture Spring for Heart Repair. *ACS Nano* **2019**, *13* (12), 14122−14137.
(36) Yu, R.; Zhang, H. L.; Guo, B. L. Conductive Biomaterials as Bioactive Wound Dressing for Wound Healing and Skin Tissue Engineering. *Nano-Micro Lett.* **2022**, *14*, 1.
(37) Maleki, A.; He, J. H.; Bochani, S.; Nosrati, V.; Shahbazi, M. A.; Guo, B. L. Multifunctional Photoactive Hydrogels for Wound Healing Acceleration. *ACS Nano* **2021**, *15* (12), 18895−18930.
(38) Wu, Y. B.; Guo, B. L.; Ma, P. X. Injectable Electroactive Hydrogels Formed *via* Host-Guest Interactions. *ACS Macro Lett.* **2014**, *3* (11), 1145−1150.
(39) Yin, J.; Han, Q. Y.; Zhang, J. C.; Liu, Y. X.; Gan, X. Q.; Xie, K. N.; Xie, L.; Deng, Y. MXene-Based Hydrogels Endow Polyetheretherketone with Effective Osteogenicity and Combined Treatment of Osteosarcoma and Bacterial Infection. *ACS Appl. Mater. Interfaces* **2020**, *12* (41), 45891−45903.
(40) Liang, Y. Q.; Li, Z. L.; Huang, Y.; Yu, R.; Guo, B. L. Dual-Dynamic-Bond Cross-Linked Antibacterial Adhesive Hydrogel Sealants with On-Demand Removability for Post-Wound-Closure and Infected Wound Healing. *ACS Nano* **2021**, *15* (4), 7078−7093.
(41) Zhu, S. J.; Yu, C. J.; Liu, N. B.; Zhao, M. Y.; Chen, Z. R.; Liu, J.; Li, G.; Huang, H. L.; Guo, H. M.; Sun, T. C. Injectable Conductive Gelatin Methacrylate/Oxidized Dextran Hydrogel Encapsulating Umbilical Cord Mesenchymal Stem Cells for Myocardial Infarction Treatment. *Bioact. Mater.* **2022**, *13*, 119−134.
(42) Zhang, W.; Pan, Z. H.; Yang, F. K.; Zhao, B. X. A Facile *in Situ* Approach to Polypyrrole Functionalization Through Bioinspired Catechols. *Adv. Funct. Mater.* **2015**, *25* (10), 1588−1597.
(43) Huang, Y.; Zhao, X.; Zhang, Z. Y.; Liang, Y. P.; Yin, Z. H.; Chen, B. J.; Bai, L.; Han, Y.; Guo, B. L. Degradable Gelatin-Based IPN Cryogel Hemostat for Rapidly Stopping Deep Noncompressible Hemorrhage and Simultaneously Improving Wound Healing. *Chem. Mater.* **2020**, *32* (15), 6595−6610.
(44) Li, P. P.; Jin, Z. Y.; Peng, L. L.; Zhao, F.; Xiao, D.; Jin, Y.; Yu, G. H. Stretchable All-Gel-State Fiber-Shaped Supercapacitors Enabled by Macromolecularly Interconnected 3D Graphene/Nanostructured Conductive Polymer Hydrogels. *Adv. Mater.* **2018**, *30* (18), 1800124.
(45) Li, P. P.; Jin, Z. Y.; Qian, Y. M.; Fang, Z. W.; Xiao, D.; Yu, G. H. Probing Enhanced Site Activity of Co-Fe Bimetallic Subnanoclusters Derived from Dual Cross-Linked Hydrogels for Oxygen Electrocatalysis. *ACS Energy Lett.* **2019**, *4* (8), 1793−1802.
(46) Chen, X. Y.; Chen, C.; Zhang, Z. J.; Xie, D. H. Gelatin-Derived Nitrogen-Doped Porous Carbon *via* a Dual-Template Carbonization Method for High Performance Supercapacitors. *J. Mater. Chem. A* **2013**, *1* (36), 10903−10911.
(47) Kedir, C. N.; Salinas-Torres, D.; Quintero-Jaime, A. F.; Benyoucef, A.; Morallon, E. Hydrogels Obtained from Aniline and Piperazine: Synthesis, Characterization and Their Application in Hybrid Supercapacitors. *J. Mol. Struct.* **2022**, *1248* (15), 131445.
(48) Liang, Y. P.; Li, M.; Yang, Y. T.; Qiao, L. P.; Xu, H. R.; Guo, B. L. pH/Glucose Dual Responsive Metformin Release Hydrogel Dressings with Adhesion and Self-Healing *via* Dual-Dynamic Bonding for Athletic Diabetic Foot Wound Healing. *ACS Nano* **2022**, *16* (2), 3194−3207.
(49) Gan, D. L.; Han, L.; Wang, M. H.; Xing, W. S.; Xu, T.; Zhang, H. P.; Wang, K. F.; Fang, L. M.; Lu, X. Conductive and Tough Hydrogels Based on Biopolymer Molecular Templates for Controlling *in Situ* Formation of Polypyrrole Nanorods. *ACS Appl. Mater. Interfaces* **2018**, *10* (42), 36218−36228.
(50) Chalmers, E.; Lee, H.; Zhu, C.; Liu, X. Q. Increasing the Conductivity and Adhesion of Polypyrrole Hydrogels with Electropolymerized Polydopamine. *Chem. Mater.* **2020**, *32* (1), 234−244.
(51) Xu, Z. J.; Han, S. Y.; Gu, Z. P.; Wu, J. Advances and Impact of Antioxidant Hydrogel in Chronic Wound Healing. *Adv. Healthcare Mater.* **2020**, *9* (5), 1901502.
(52) Mao, L.; Wang, L.; Zhang, M. Y.; Ullah, M. W.; Liu, L.; Zhao, W. W.; Li, Y.; Ahmed, A. A. Q.; Cheng, H. Y.; Shi, Z. J.; Yang, G. *In Situ* Synthesized Selenium Nanoparticles-Decorated Bacterial Cellulose/Gelatin Hydrogel with Enhanced Antibacterial, Antioxidant, and Anti-Inflammatory Capabilities for Facilitating Skin Wound Healing. *Adv. Healthcare Mater.* **2021**, *10* (14), 2100402.
(53) Zhou, T.; Xiong, H.; Wang, S. Q.; Zhang, H. L.; Zheng, W. W.; Gou, Z. R.; Fan, C. Y.; Gao, C. Y. An Injectable Hydrogel Dotted with Dexamethasone Acetate-Encapsulated Reactive Oxygen Species-

https://doi.org/10.1021/acsnano.2c05557
ACS Nano 2022, 16, 13022−13036

Scavenging Micelles for Combinatorial Therapy of Osteoarthritis. *Mater. Today Nano* **2022**, *17*, 100164.
(54) Wang, Y. L.; Jiang, B.; Sun, T.; Wang, S.; Jin, Y. C. A Bio-Inspired MXene/Quaternary Chitosan Membrane with a "Brick-and-Mortar" Structure Towards High-Performance Photothermal Conversion. *J. Mater. Chem. C* **2022**, *10* (20), 8043−8049.
(55) Ghomi, E. R.; Khalili, S.; Khorasani, S. N.; Neisiany, R. E.; Ramakrishna, S. Wound Dressings: Current Advances and Future Directions. *J. Appl. Polym. Sci.* **2019**, *136* (27), 47738.
(56) Chen, J. Y.; He, J. H.; Yang, Y. T.; Qiao, L. P.; Hu, J.; Zhang, J.; Guo, B. L. Antibacterial Adhesive Self-Healing Hydrogels to Promote Diabetic Wound Healing. *Acta Biomater.* **2022**, *146*, 119−130.
(57) Liang, Y. P.; Li, M.; Huang, Y.; Guo, B. L. An Integrated Strategy for Rapid Hemostasis during Tumor Resection and Prevention of Postoperative Tumor Recurrence of Hepatocellular Carcinoma by Antibacterial Shape Memory Cryogel. *Small* **2021**, *17* (38), 2101356.
(58) Gulfam, M.; Jo, S. H.; Jo, S. W.; Vu, T. T.; Park, S. H.; Lim, K. T. Highly Porous and Injectable Hydrogels Derived from Cartilage Acellularized Matrix Exhibit Reduction and NIR Light Dual-Responsive Drug Release Properties For Application in Antitumor Therapy. *NPG Asia Mater.* **2022**, *14* (1), 8.
(59) Fang, K.; Wang, R.; Zhang, H.; Zhou, L. J.; Xu, T.; Xiao, Y.; Zhou, Y.; Gao, G. R.; Chen, J.; Liu, D. L.; Ai, F. R.; Fu, J. Mechano-Responsive, Tough, and Antibacterial Zwitterionic Hydrogels with Controllable Drug Release for Wound Healing Applications. *ACS Appl. Mater. Interfaces* **2020**, *12* (47), 52307−52318.
(60) Guedes, G.; Wang, S. Q.; Fontana, F.; Figueiredo, P.; Linden, J.; Correia, A.; Pinto, R. J. B.; Hietala, S.; Sousa, F. L.; Santos, H. A. Dual-Crosslinked Dynamic Hydrogel Incorporating $\{Mo_{154}\}$ with pH and NIR Responsiveness for Chemo-Photothermal Therapy. *Adv. Mater.* **2021**, *33* (40), 2007761.
(61) Wang, X. D.; Meier, R. J.; Wolfbeis, O. S. Fluorescent pH-Sensitive Nanoparticles in an Agarose Matrix for Imaging of Bacterial Growth and Metabolism. *Angew. Chem., Int. Ed.* **2013**, *52* (1), 406−409.
(62) Zhou, W. H.; Jia, Z. J.; Xiong, P.; Yan, J. L.; Li, M.; Cheng, Y.; Zheng, Y. F. Novel pH-Responsive Tobramycin-Embedded Micelles in Nanostructured Multilayer-Coatings of Chitosan/Heparin with Efficient and Sustained Antibacterial Properties. *Mater. Sci. Eng., C* **2018**, *90*, 693−705.
(63) Zhang, H.; Sun, X. Y.; Wang, J.; Zhang, Y. L.; Dong, M. N.; Bu, T.; Li, L. H.; Liu, Y. N.; Wang, L. Multifunctional Injectable Hydrogel Dressings for Effectively Accelerating Wound Healing: Enhancing Biomineralization Strategy. *Adv. Funct. Mater.* **2021**, *31* (23), 2100093.
(64) Huang, S. C.; Xu, S. B.; Hu, Y. A.; Zhao, X. J.; Chang, L. N.; Chen, Z. H.; Mei, X. F. Preparation of NIR-Responsive, ROS-Generating and Antibacterial Black Phosphorus Quantum Dots for Promoting the MRSA-Infected Wound Healing in Diabetic Rats. *Acta Biomater.* **2022**, *137*, 199−217.
(65) Cao, C. Y.; Ge, W.; Yin, J. J.; Yang, D. L.; Wang, W. J.; Song, X. J.; Hu, Y. L.; Yin, J.; Dong, X. C. Mesoporous Silica Supported Silver-Bismuth Nanoparticles as Photothermal Agents for Skin Infection Synergistic Antibacterial Therapy. *Small* **2020**, *16* (24), 2000436.
(66) Elmassry, M. M.; Mudaliar, N. S.; Colmer-Hamood, J. A.; San Francisco, M. J.; Griswold, J. A.; Dissanaike, S.; Hamood, A. N. New Markers for Sepsis Caused by *Pseudomonas aeruginosa* During Burn Infection. *Metabolomics* **2020**, *16* (3), 40.
(67) Liang, Y. P.; Zhao, X.; Hu, T. L.; Chen, B. J.; Yin, Z. H.; Ma, P. X.; Guo, B. L. Adhesive Hemostatic Conducting Injectable Composite Hydrogels with Sustained Drug Release and Photothermal Antibacterial Activity to Promote Full-Thickness Skin Regeneration During Wound Healing. *Small* **2019**, *15* (12), 1900046.
(68) Xiao, J.; Zhou, Y. J.; Ye, M. Q.; An, Y.; Wang, K. N.; Wu, Q. J.; Song, L. W.; Zhang, J. W.; He, H. C.; Zhang, Q. W.; Wu, J. Freeze-Thawing Chitosan/Ions Hydrogel Coated Gauzes Releasing Multiple Metal Ions on Demand for Improved Infected Wound Healing. *Adv. Healthcare Mater.* **2021**, *10* (6), 2001591.
(69) Liang, Y. P.; He, J. H.; Guo, B. L. Functional Hydrogels as Wound Dressing to Enhance Wound Healing. *ACS Nano* **2021**, *15* (8), 12687−12722.
(70) Li, M.; Liang, Y. P.; Liang, Y. Q.; Pan, G. Y.; Guo, B. L. Injectable Stretchable Self-Healing Dual Dynamic Network Hydrogel as Adhesive Anti-Oxidant Wound Dressing for Photothermal Clearance of Bacteria and Promoting Wound Healing of MRSA Infected Motion Wounds. *Chem. Eng. J.* **2022**, *427*, 132039.
(71) Zhao, X.; Zhang, Z. Y.; Luo, J. L.; Wu, Z. Y.; Yang, Z. F.; Zhou, S. W.; Tu, Y. P.; Huang, Y.; Han, Y.; Guo, B. L. Biomimetic, Highly Elastic Conductive and Hemostatic Gelatin/rGO-Based Nanocomposite Cryogel to Improve 3D Myogenic Differentiation and Guide *in Vivo* Skeletal Muscle Regeneration. *Appl. Mater. Today* **2022**, *121*, 101365.
(72) Hu, J. J.; Hu, Q. Y.; He, X.; Liu, C. X.; Kong, Y. L.; Cheng, Y. Y.; Zhang, Y. D. Stimuli-Responsive Hydrogels with Antibacterial Activity Assembled from Guanosine, Aminoglycoside, and a Bifunctional Anchor. *Adv. Healthcare Mater.* **2020**, *9* (2), 1901329.
(73) Huang, Y.; Zhao, X.; Wang, C. B.; Chen, J. Y.; Liang, Y. Q.; Li, Z. L.; Han, Y.; Guo, B. L. High-Strength Anti-Bacterial Composite Cryogel for Lethal Noncompressible Hemorrhage Hemostasis: Synergistic Physical Hemostasis and Chemical Hemostasis. *Chem. Eng. J.* **2022**, *427*, 131977.
(74) Yuan, Y.; Shen, S. H.; Fan, D. D. A Physicochemical Double Cross-Linked Multifunctional Hydrogel for Dynamic Burn Wound Healing: Shape Adaptability, Injectable Self-Healing Property and Enhanced Adhesion. *Biomaterials* **2021**, *276*, 120838.

https://doi.org/10.1021/acsnano.2c05557
ACS Nano 2022, 16, 13022−13036